A NATURAL ORIGIN FOR ARSENIC AND IRON RICH SEEPS FROM A CHALK IN THE VICINITY OF UNLINED LANDFILLS, NORTH-CENTRAL TEXAS, USA

by

Jackie D. Horn

APPROVED BY SUPERVISORY COMMITTEE:

_____

Dr. Thomas H. Brikowski, Chair

_____

Dr. Robert Finkelman

_____

Dr. William R. Griffin

To all the people who let me dream and aspire to becoming the scientist that I wanted to become. Without everyone's constant support and wisdom, I would have been doomed to the cycle of ignorance and pain. Thank you for simply believing in me.

A NATURAL ORIGIN FOR ARSENIC AND IRON RICH SEEPS FROM A CHALK IN THE VICINITY OF UNLINED LANDFILLS, NORTH-CENTRAL TEXAS, USA

by

JACKIE D. HORN, B.S.

DISSERTATION

Presented to the Faculty of

The University of Texas at Dallas

in Partial Fulfillment

of the Requirements

for the Degree of

MASTER OF SCIENCE IN

GEOSCIENCES

THE UNIVERSITY OF TEXAS AT DALLAS

December 2018

ACKNOWLEDGMENTS

I would like to acknowledge Dr. Tom Brikowski, Dr. Ignacio Pujana, Dr. Robert Finkelman, Dr. Randy Griffin, Dr. Matthew Loocke, Dr. Robert J. Stern, Dr. John Giessman, Dr. George McMechan, and Dr. James L. Carter for their continued guidance and patience. Without the lessons they taught me, I would not be here. Many thanks for the excellent editing advice that my editors, Leah Thompson, April Allen Langhans, and Julia McIntosh, provided and their continued awesomeness. Thanks to all parties (University Texas at Arlington Shimatzu Lab, Micro Imaging Lab, and the City of Richardson) that provided the means for completion of this work. Gratitude and thanks for all the many field hands who helped with acquisition of data and manual labor. Without the support of UTD Geosciences Department and The University of Texas at Dallas there would not be a thesis.

December 2018

A NATURAL ORIGIN FOR ARSENIC AND IRON RICH SEEPS FROM A CHALK IN THE VICINITY OF UNLINED LANDFILLS, NORTH-CENTRAL TEXAS, USA

Jackie D. Horn, B.S
The University of Texas at Dallas, 2018

Supervising Professor: Thomas H. Brikowski, PhD

Seepage of suspicious iron, arsenic and sulfur rich waters from streambanks down-gradient from unlined landfills in North Texas has led to sharp public concern. Seep waters exhibit somewhat low pH (6.3), reduced state (Eh = -100 mV), high iron (40 ppm), elevated arsenic (105 ppb), barium (634 ppb), manganese (3 ppm), bromine (9 ppm), and salinity (TDS = 1380 ppm), an iridescent sheen and sulfurous odor. Bright orange colloids precipitate soon after the seeps emerge from the streambank, reminiscent of acid mine drainage. Other indicators of landfill leachate are absent, however, e.g., elevated Cr-Pb-Zn-Cu, PAHs.

Ample natural sources of iron and arsenic are present. The bedrock is Cretaceous chalk, and SEM/microprobe analysis reveals considerable pyritization of foraminifera tests, with framboidal texture indicating microbial deposition. These diagenetic sulfide grains were subsequently altered to iron oxyhydroxides ($FeOOH_x$). Electron microprobe profiles reveal primarily iron and sulfur in the original grains, and primarily iron in the weathered rinds. Arsenic is distributed evenly in both phases, but is absent in surrounding carbonate. Presumably, dissolution of the

$FeOOH_x$ simultaneously releases iron and arsenic to form the seep discharge. Reducing acidic conditions (e.g., acid mine drainage or landfill leachate contribution from up-gradient landfills) allow this breakdown and transport. As a result, further sulfide minerals may breakdown as conditions transition from a reducing to oxidizing environment (e.g., shallow aquifer and surficial weathering) creating a positive feedback loop to sulfide decay. Some type of microbial seeding from the landfills may explain their spatial association with apparently natural Fe-rich seeps.

TABLE OF CONTENTS

LIST OF FIGURES

LIST OF TABLES

CHAPTER 1

INTRODUCTION

1.1 Purpose and Objectives

Striking orange-colored iron, arsenic and sulfur rich waters are oozing from streambanks down-gradient from unlined landfills in North Texas. It is crucial to determine their origin for allaying, or confirming, public concerns and identifying possible remediation. Possible sources include leaching of anthropogenic constituents from the landfill or leaching of natural components such as iron sulfide grains, from the associated Austin Chalk. These microscopic grains of pyrite are uniformly distributed throughout the formation. Scanning Electron Microscopy (SEM) with Energy Dispersive X-Ray Spectrometry (EDS) sheds some light on the past and present biogenic processes forming and altering these sulfides. The landfill contribution may be indirect, since other settings landfill leachate contributions have been found to activate local microbe populations thus enabling the reduction of biogenic iron (Fe, Saunders et al. 1997). Indeed, field samples of the seeps indicate strongly reducing (i.e., less oxygen available) and mildly acidic groundwater conditions in the bedrock. The seeps exhibit moderately elevated salinity (total dissolved solids, TDS, of 800-1400 ppm, parts per million), are surprisingly acidic (6.1-6.6), considering the carbonate host rock and have minimal turbidity at the orifice (1.07 NTU, Nephelometric Turbidity Units). The high arsenic (105 parts per billion (ppb, As) and mercury (5.2 ppb (Hg)) may indicate anthropogenic origins, but other typical landfill leachate metals (Cd, Cr, Pb, Se, Ag; Resource Conservation and Recovery Act or RCRA-8; EPA 2018, Kjeldsen et al., 2002) are well below regulatory limits. The discharge emerges as clear, but rapidly

precipitates bright orange Fe-colloids upon reaction with the atmosphere, reflecting high Fe content (16.4 ppm) of the seeps. Aqueous transport of this Fe and accompanying metals is a dynamic subsurface process accomplished by geo-microbial breakdown of the original sulfides (Lovely and Phillips 1988), and is the predominant control on trace element cycling in the study area.

The close proximity of these prominent seeps to now-abandoned landfills, combined with their striking orange color, iridescent sheen and a sulfurous odor, have combined to lead local residents to suspect an industrial origin for the leachate. A single sample analyzed by environmental authorities, Texas Commission of Environmental Quality (TCEQ), suggested little hazard, finding elevated, but below drinking-water standard levels of Arsenic (As) and only moderately elevated iron. However, this could be due to improper collection of sample of post-precipitation water, which would show reduced levels of As and Fe due to dilution with rain water. Involvement of academic researchers (university faculty) led to discovery of similar discharge in a nearby creek, Rowlett Creek, below another abandoned landfill (Breckenridge Park), motivating this investigation into a potentially more general phenomenon.

1.2 Study Location and Landfill History

This study focuses on two sites in North Dallas (Figure 1), both exhibiting seepage that is visually reminiscent of acid mine drainage (Figure 2). The primary study site (with the best access) is Spring Creek in Richardson, TX (Figure 3a), and the second is Rowlett Creek (Figure 3b), both hydraulically down gradient from now-abandoned unlined landfills.

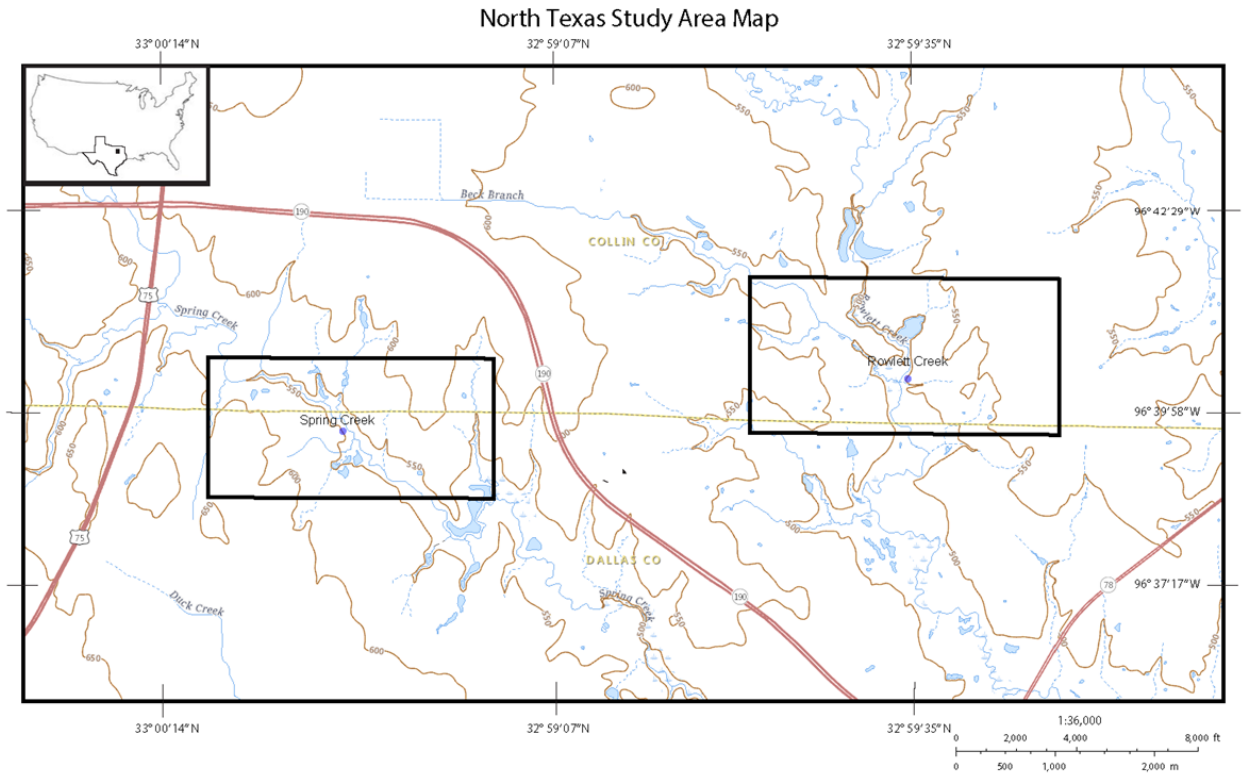

Figure 1: Study areas in North Texas, Dallas-Fort Worth Metroplex, TX U.S.A., showing the two locales on adjacent major creeks (Spring Creek, Figure 2a, and Rowlett Creek, Figure 2b) in the highlighted boxes that were the principal research areas for Iron discharge zones in the Austin Chalk.

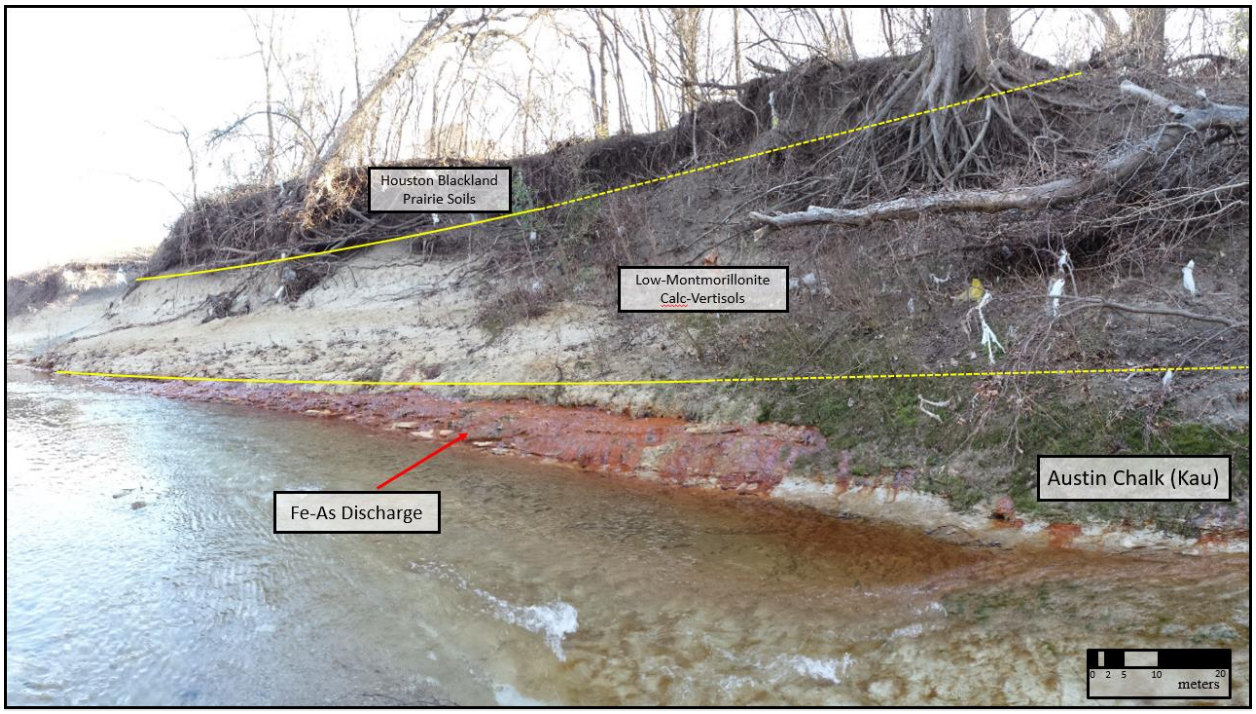

Figure 2: Spring Creek south bank (Figure 3a, point B) showing reddish-brown discharge zone. Three horizons identified as Houston Blackland prairie soils on top of low montmorillonite vertisols and transitions into a bleached/leached calcisol with mottles that have some characteristics of a gleysol that primarily fills paleochannels on top of the bedrock chalk. Deposits are from a meandering stream channel. Note that although contacts are drawn straight (yellow line) they are U-shaped. The Fe-As rich discharge emerges from the contact between the calc-vertisol layer and exposed Austin Chalk.

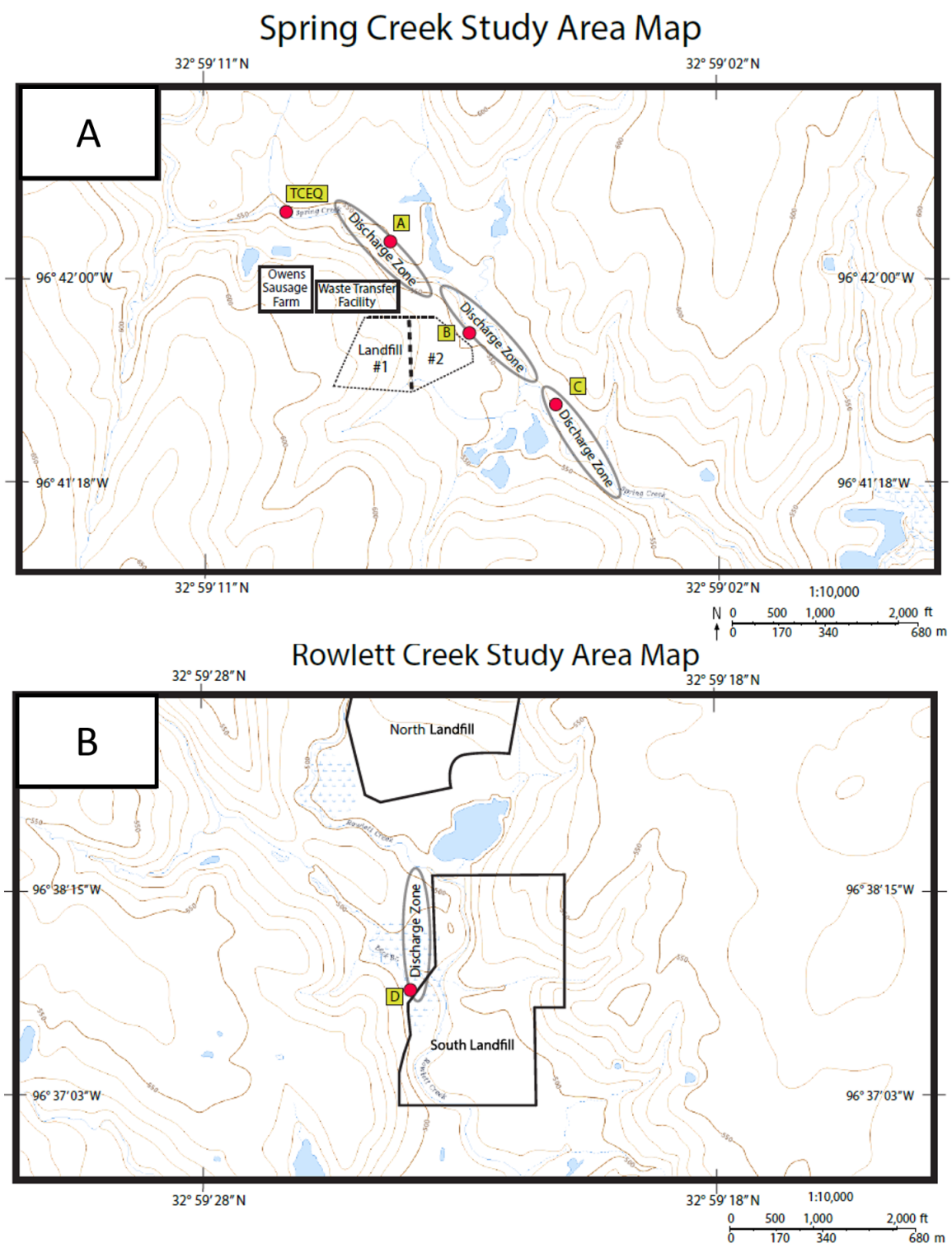

Figure 3: A) Primary study area in Richardson, TX along Spring Creek (14S E715439 N3651791). Water chemistry monitored at sample points A-C over two-year period, and previous single-sample study (TCEQ, 2009); approximate locations of landfills shown in dashed lines with interpreted boundary between #1 and # 2. Potential waste sources indicated by boxes. B) Secondary study area in Richardson, TX (14S E722136 N3653656) along Rowlett Creek. Water chemistry samples collected at point D. Location of closed landfills is based on records from NCTCOG (www.nctcog.org).

The landfills in the study area are old (begun in the 1950's, closed 20-30 years later), and are unlikely to have been lined, which raises the possibility of contribution to the seeps from anthropogenic sources. Study area 1 was a borrow pit in a gully that was subsequently converted to a landfill, and area 2 was probably developed when area 1 was filled. The Spring Creek site is now occupied by a golf course and athletic fields/park; the Rowlett Creek site is now athletic fields. Little construction information is available for the landfills, but their vintage indicates no liner material or engineered cap was installed. Both are thinly capped with local montmorillonite-rich vertisol material and are irrigated to varying degrees. Materials in the landfills are likely to be typical of small agrarian-focused towns, e.g., farm equipment and some household waste. The official landfill area is 63 - 66 acres, presumably evenly divided between the two landfills (see Figure 3a: Landfill 1 and Landfill 2). The Rowlett Creek site also contains two known landfills (North and South in Figure 3b). The landfill area in total is 90 - 100 acres (North is 40 – 50 and South is 35 – 40), and, landfills were capped with clay and then converted into Breckenridge Park athletic fields. Observed seeps at this site were near the south landfill, and much of the seep area is accessible only by boat.

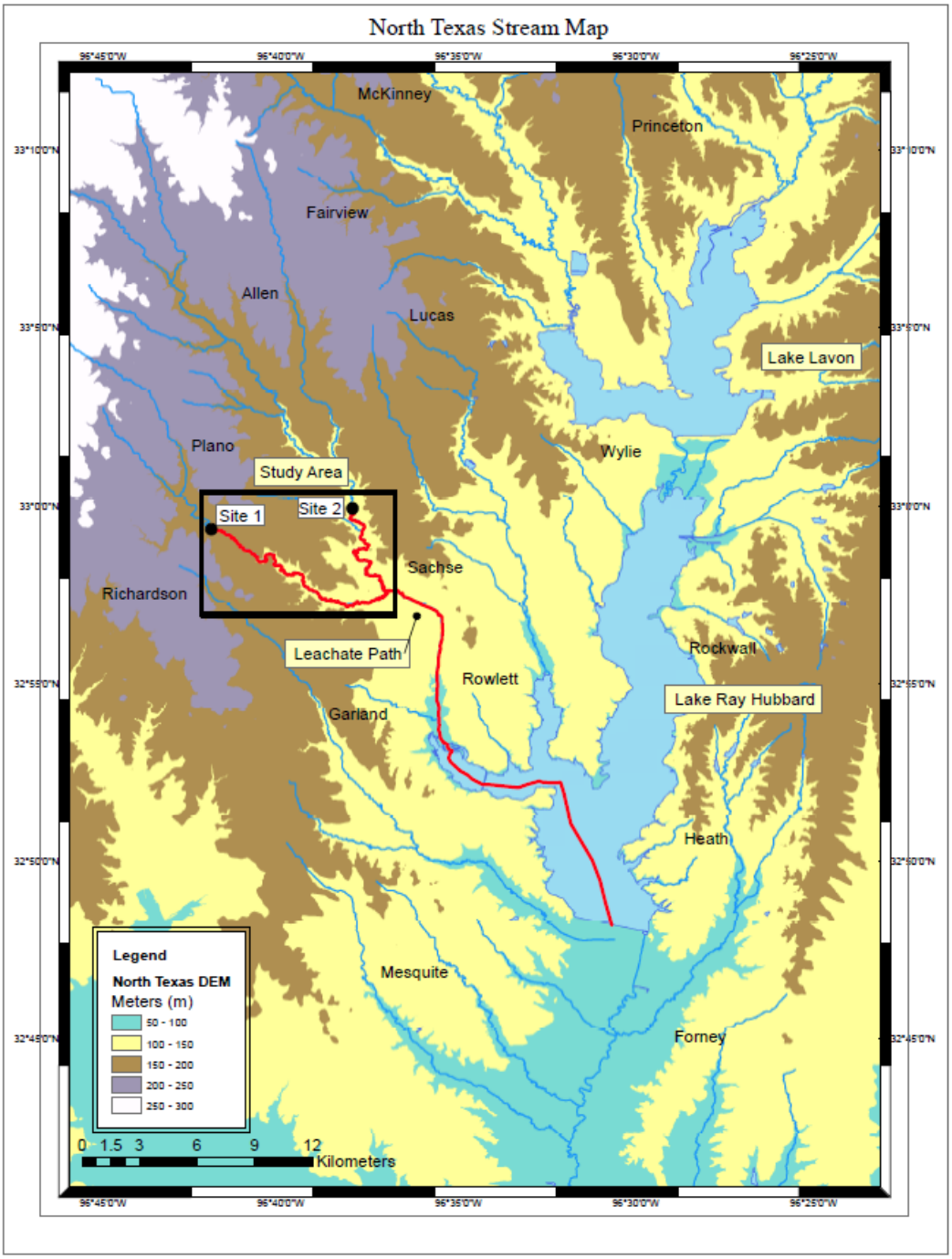

Figure 4: North Texas Stream Map showing the extent of study area shown in Figure 1. Red line indicates the flow path for the Fe-As discharge zones along Spring Creek and Rowlett Creek and terminate with final mixing in Lake Ray Hubbard. Site 1 and 2 refer to study areas in Figure 2a and Figure 2b.

1.3 Discharge Zones

The discharge zones analyzed in this study appear intermittently along outcrops of the Cretaceous Austin Chalk (Figure 2) and represent laterally extensive areas of sluggish reddish-brown discharge. Discharge zones occupy a 1-2-kilometer (km) exposure along the banks of Spring and Rowlett Creeks. Each zone is 100-200 meters (m) in length, containing multiple seeps 3 to 10 m in length with concentrated flow. At both locations, discharge is predominantly on the same bank as the landfill, but minor occurrences can be found on the opposite bank at Spring Creek, and also occur upstream, but not necessarily up groundwater gradient from the landfill. The seep emerges at the contact between the base of soil (cal-vertisol layer) and bedrock (Kau, Figure 2). Both site locations streams flow to the southeast and the final flow path of the As-Fe discharge terminates with final mixing into Lake Ray Hubbard (Figure 4).

CHAPTER 2

RESEARCH METHODS

2.1 Overview

Water, soil, and rock samples were collected over a period of two years for analysis to determine the nature of the seeps. The water samples from seep orifice were analyzed to find the concentration of dissolved cations, anions, organics, and trace metals present to understand the provenance of the fluids. Soil samples were taken to determine the stratigraphy and mineralogy of the stream banks. Bedrock samples were analyzed via thin section to determine if it could be a local source of iron and to determine the origin of elevated arsenic.

2.2 SEM/Microprobe Thin Section Sample Preparation:

Rock samples of the Austin Chalk were collected around Spring Creek discharge zones (A, B, and C, Figure 3a). Polished sections for SEM analysis were prepared by a commercial laboratory. The samples were oriented so that the polished surface lay along a bedding plane. The sections measured 46 x 27 mm with single polish (thickness (T) of 0.05 µm and base (B) of 3 µm); carbonate stain (Alizarin red stain (ARS) + potassium ferricyanide (PF)), clear epoxy impregnation, and preparation using oil to avoid sample dissolution.

Preliminary selection of points of interest (POI) was made with a Leica 750D transmitted and reflected light petrologic microscope. The POI's were chosen to evaluate (iron) oxidized zones

visible in thin section. Analysis of these POI was carried out with a JEOL JSM-IT200 SEM, with thin section mounted on to a 10 mm brass plug with double-sided carbon tape to affix slide. The settings chosen for the analysis: working distance (WD) of 10 mm and beam height of 17 mm for best images. The sample is conductive and therefore the low vacuum (LV) and inorganic setting were applied for backscatter detector (BES) characterization. To ensure that charging of the sample was minimal a range of 10 to 15 kiloelectron volts (keV) were used. Images and geochemical data were acquired from secondary electrons to render an EDS map of the POI.

Once a POI has been located then the EDS collection to generate a chemical map of the composition proceeded. Single point analysis was used to verify the content of Fe, S, O, and Ca in each POI to distinguish between various minerals. Data presented is in oxides and element percentages where necessary.

Analysis of POI was carried out with an EPMA-1720HT Electron Probe Microanalyzer. Around 100 points of data were collected from various oxides and sulfides in three thin sections picked to mirror the POI in the SEM analysis. Beam conditions were set to have a spot size of 1 μm, voltage at 15 kV and beam current at 20 nanoamps (nA). The dwell time for each spot was 20 seconds and the machine ran for 6 - 8 hours to acquire data. Oxides and sulfides values were checked based on standards for pyrite and magnetite. The data collected was in concentrations of weight percent of selected elements (Fe, S, As, Ti, Mg, Mn, Ca, C, Br, and O) and then normalized. All values were obtained from K alpha (α) shells, except arsenic and bromine, which we from the Lα shell.

2.3 Water Sampling and Analysis:

United States Geological Survey (USGS), EPA, and WHO water collection standards and practices guided our collection, storage and analysis of the samples. Three 250 ml high density polyethylene (HDPE) bottles of water (or leachate) were collected, one for cations filtered and preserved with 0.5 milliliter (mL) of nitric acid (HNO_3) to bring the pH to less than 2, and two bottles unfiltered and unpreserved for anion and additional cation analysis. Each sample was collected directly at the spring orifice using a clean 60 mL syringe, with a 0.45-micrometer (µm) filter. A new syringe was utilized at each sample site. A blank sample of deionized water (DI) was collected at each site as well. All samples were labeled and stored on ice in a cooler in the field. Samples were refrigerated in the lab until sent (refrigerated on ice) to outside labs for analysis. Temperature (C°), Total dissolved solids (TDS), pH, dissolved oxygen (DO), specific conductance (µS/m), and turbidity (NTU) were measured in the field at the time of collection.

CHAPTER 3

NATURE OF LEACHATE

3.1 Groundwater (Spring) Geochemistry

Rapid stream erosion along the outside curve of meanders produce steep banks in the bedrock that locally intersect the water table, resulting in springs fed by the alluvial aquifer. Away from the apparent leachate seeps, the composition of the waters coming out of the springs in the research areas is very similar to the creek waters (and to the Fe-seeps after they've precipitated the dissolved iron). The leachate seeps typically produce gelatinous orange Fe-oxyhydroxide deposits that coat stream banks. The same material appears in unpreserved samples within a few hours of collection. SEM-EDS analysis of that precipitate after dehydration showed 46.8 % Fe, and ICP-MS showed 0.1 ppm Mn, 0.18 ppm Ba, and 8 ppb As. Preserved samples from the spring orifice contain appreciable dissolved iron, manganese, and possibly other trace metals (Spring Creek sample, Table 1), while samples taken along the seep path down the streambank show declining TDS and increasing pH (Figure 5) which might account for decline in Fe. In major element composition the seeps are consistent with meteoric water in contact with the Austin Chalk and are dominantly calcium bicarbonate ($Ca(HCO_3)_2$) waters. TDS is elevated (850 - 1308 ppm) and has pH values from 6.2 to 6.4. The typical composition of the nearby streams is 300 - 400 TDS and pH of 7.1 - 8. Low Na (85 – 92 ppm) and Cl (142 – 390 ppm) indicate that the seep waters are distinct from formation fluids (Na; 10000 – 20000 ppm and Cl; 20000 - 35000 ppm) and most likely originate in a shallow aquifer.

Table 1: Groundwater chemical data collected for Spring Creek and Rowlett Creek seeps at the spring orifice.

Chemical Analyses of Seep Water (mg/L Except as Noted)		
	Spring Creek	Rowlett Creek
As	0.105	0.00431
Fe	16.4	41.1
Mn	0.563	3.34
Pb	< 0.003	< 0.003
Ca	235	282
K	40.2	9.87
Mg	20.4	11.5
Na	92.3	85.9
Cl	142	390
SO_4	7.54	21.8
Alkalinity (as $CaCO_3$)	754	448
Field Measurements		
TDS	1308	850
pH (std. units)	6.2	6.4
Specific Conductance ($\mu S\ cm^{-1}$)	618	825
Temperature (C°)	21.1	23.1

A reaction study of Eh-pH along the path of the fluids emerging from the spring to the stream shows an overall trend of reducing conditions in the subsurface rapidly becoming oxidized after emergence (Figure 5). Upon emergence, the TDS of seep water is high (~900 ppm) and quickly decreases as it flows down the bank, becoming more oxygenated. Immediately before entering the stream, TDS reaches typical stream values (~300 ppm). As a result, care must be taken to sample at the spring orifice if trace metal migration in the subsurface is to be properly characterized. At the spring orifice metals typically found in landfill leachate (RCRA-8) are typically low to below-detection limit (via ICP), with the exception of As and Hg (Table 4 and Table 6).

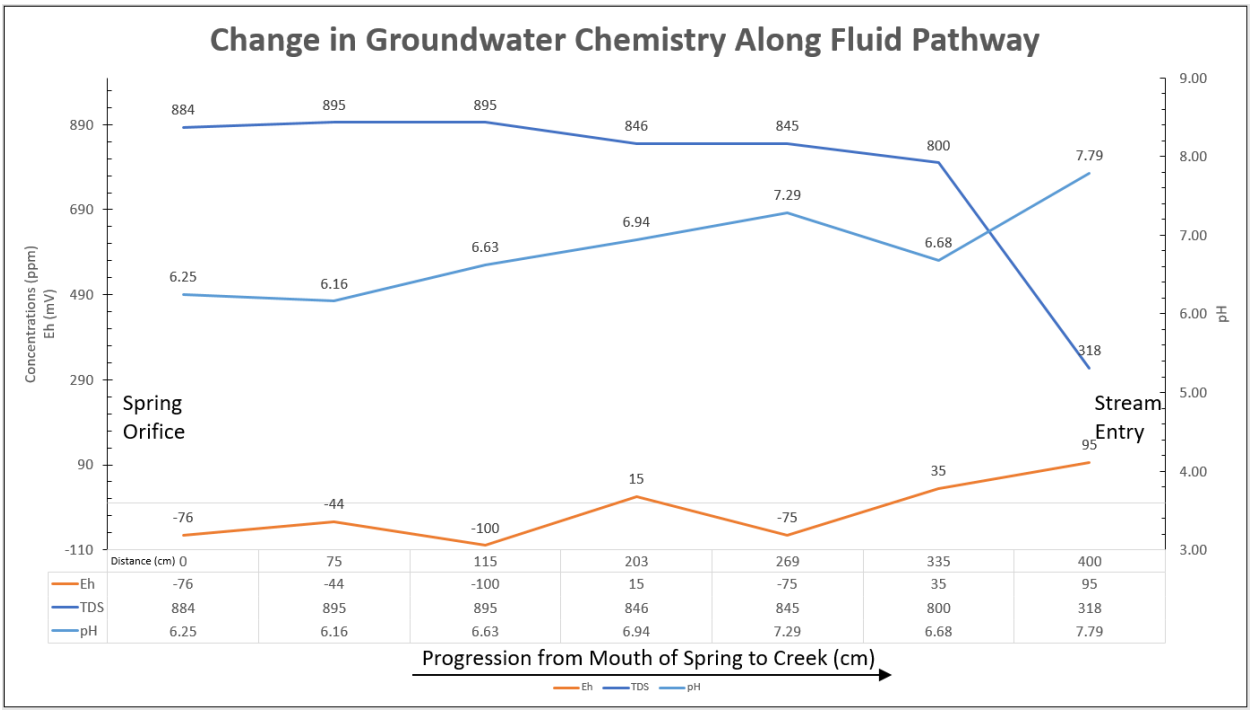

Distance (cm)	0	75	115	203	269	335	400
Eh	-76	-44	-100	15	-75	35	95
TDS	884	895	895	846	845	800	318
pH	6.25	6.16	6.63	6.94	7.29	6.68	7.79

Figure 5: Chemical progression of oxidation potential (Eh) pH, and salinity (TDS) along flow distance from spring orifice to stream entry at Spring Creek site. General trend of oxidation occuring as fluids progress to stream. Rapid Precipitation of FeOOH occurs as the Eh increases

and the bulk of the Fe-discharge is near the 1m distance from stream. Total distance is 4 m, data summarized in Table 2.

Table 2: Reaction of fluids along seepage pathway from orifice to stream, Spring Creek site.

Time Step Fluid Reaction Along Conduit Analysis		
Distance (cm)	pH	Eh (mV)
0	6.25	-76
75	6.16	-44
115	6.62	-100
203	6.94	15
269	7.29	-75
335	6.68	35
400	7.79	95

Seep and creek waters are geochemically distinct from one another, and seep waters are distinct from typical landfill leachate and formation water compositions. The seep water exhibits a weak geochemical fingerprint (calcium bicarbonate, $Ca(HCO_3)_2$) with a high Fe content (16-40 mg/L). The fact that both sites have landfills near them would suggest that some of the contribution to seeps is from the waste, but the metals and water chemistry do not argue for anthropogenic source. Results from leachates are not consistent with domestic solid waste leachate (Table 3 analyses reported in the literature: e.g., Renou et al. 2007; Apgar and Langmui, 1970; Fungaroli and Steiner, 1971; Merz, 1954; Qasim and Burchinal 1970; Williams 1974). A potential indicator of landfill contribution would be elevated concentrations of environmentally persistent

hydrocarbons such as PCB's (Table 3). Chloride and bromine, and particularly their ratio is a commonly accepted discriminant of formation vs. anthropogenic brines. In the seeps, only moderate elevation of Cl (390 mg/L) and bromine (Br 9.30 mg/L) indicates that the seeps are, at best, much-diluted landfill leachate (Panno et al., 2006). The Cl/Br ratio is 42 and the ratio does not indicate any type of landfill leachate. There were no detectable levels of pesticides, organochlorides, phosphates, phenols, Volatile Organic Compounds (VOC) or other identifiable chains. Low values of Total Organic Carbon (TOC), Biochemical Oxygen Demand (BOD), and Chemical Oxygen Demand (COD) show the maturity of the landfill and the ratio of BOD_5: COD is similar to leachate from a landfill of 20-30 years age in a methanogenic phase (Kjeldsen et al., 2002, Table 4). Landfill contribution to the sampled leachate is minimal due to age of landfill (mature), reacted organics, and only metals (Fe, As, Mn, and Hg) left to transport. For instance, anaerobic leachate exposed to oxygen may cause Fe (II) to oxidize to Fe (III) and precipitate out of the leachate resulting in the high levels of Fe.

Table 3: Analysis of Selected Inorganic and Organic Compounds, Spring Creek Sample point C in Figure 3a, compared to typical values for landfill leachate.

Inorganic and Organic Analyses of Study Seep Water (mg/L Except as Noted)		
	Spring Creek	Leachate Composition[1]
Cl/Br (ratio)[2]	42	42 - 5404
Total Kjeldahl Nitrogen (TKN)	36.6	14-2500
Nitrate-Nitrite as N	< 0.018	10 - 13000
Total Phenols	0.00517	1 - 1200
Total Suspended Solids (TSS)	56	2000- 60000
Ammonia as N	35.2	50 - 1800
Phosphate ($PO4^{3-}$)	< 0.015	0.1 - 20
Organic Matter		
Physical Biological Oxygen Demand (BOD_5)	16.2	20 - 57000
Chemical Oxygen Demand (COD)	68.1	140 - 90000
BOD_5/COD (ratio)	0.24	0.02 – 0.80
Total Carbon	293	
Total Organic Carbon (TOC)	19.5	30 - 27700
Total Dissolved Solids (TDS)	800	2000 - 60000
pH	6.1	4.5 - 9
Specific Conductance		2500 - 25000

[1] Christensen et al. 2009

[2] Panno et al. 2009

Table 4: Concentrations of RCRA-regulated metals reported for Spring Creek site, by TCEQ (Sept 2009 and Dec 2009), and Point B in Figure 3a. Concentrations in mg/L unless noted otherwise. Sample SC09 most likely taken at base of seep, after most iron and metals had precipitated.

RCRA Analyses of Study Water (mg/L Except as Noted)				
	SC09	SC17	Leachate Composition[3][4][5]	EPA Limits[6][7]
Arsenic (As)	1.49	0.105	0.01 - 1	0.010
Barium (Ba)	2.07	0.634	0.01 – 0.5	2.00
Cadmium (Cd)	< 0.0003	< 0.0003	0.0001 – 0.4	0.005.0
Chromium (Cr)	0.021	0.00127	0.02 – 1.5	0.1
Coper (Cu)	0.041	< 0.005	0.005 - 10	1.3
Lead (Pb)	0.026	< 0.0003	0.001 - 5	0.015
Manganese (Mn)	7.27	3.34	0.03 - 1400	0.05
Nickel (Ni)	0.061	0.00362	0.015 - 13	0.1
Selenium (Se)	< 0.004	< 0.004	0.05 - 0.1	0.05
Silver (Au)	< 0.001	< 0.0041	0.035	0.10
Zinc (Zn)	0.184	0.00612	0.03 - 1000	3.0

[3] Christensen et al. 2009, Heavy Metals.

[4] After USEPA, 1991b, USEPA, 2001.

[5] Plotkin and Ram 1984, Barium.

[6] EPA Safe Water Drinking Limits.

[7] WHO Chemical Hazards in Drinking Water.

CHAPTER 4

RESULTS

4.1 Origin of Leachate

The most important question regarding the seeps is the origin of the prominent iron and associated colloids and staining. Of specific concern to the public is the origin of toxic metals that may accompany that iron, and the reason for the apparent spatial correlation of seeps with unlined landfills. From looking a multitude of realms (biologic, chemical, and physical) we are able to gain a better understanding of the dynamic cycle (Figure 6) responsible for the transport of arsenic and iron in these seeps. For that, first a detailed textural and chemical analysis of alteration the Austin Chalk bedrock is required, followed by correlation of characterization of municipal waste landfill leachate and compare with this studies anomalous concentration in the seep waters.

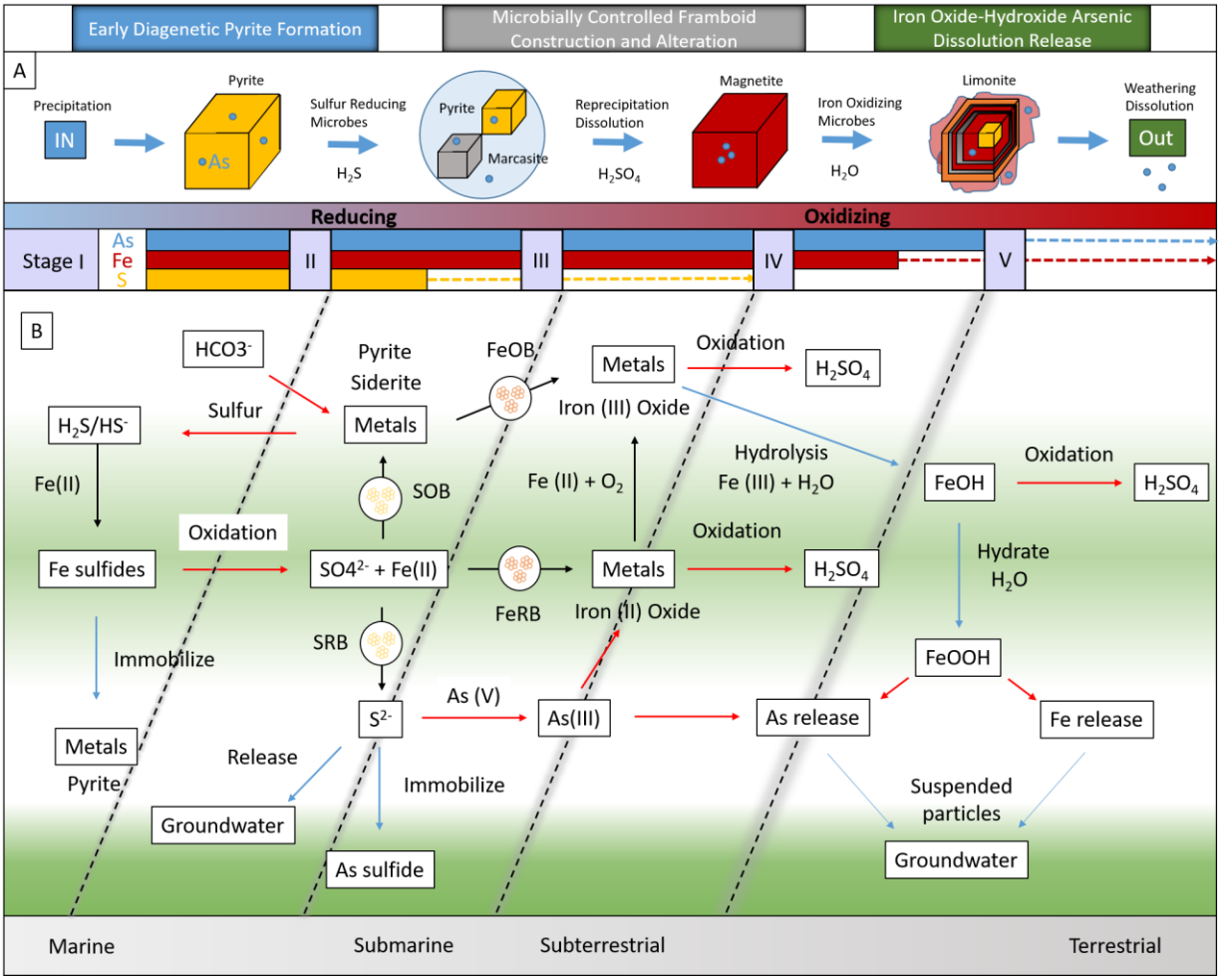

Figure 6: Complete cycle of Fe-As transport and release in Austin Chalk. Stage I is the early formation of pyrite (inorganic and organic reactions) and the incorporation of arsenic in the mineral. Stage II results from sulfur reducing microbe's facilitating in the pyrite decay cycle. Stage III is the start of reprecipitation-dissolution of sulfides to oxides, small loss of sulfur commences and the secondary formation of Fe-sulfide minerals form. The acid that is released in the pyrite-marcasite decay lowers the pH and helps in the dissolution of siderite and sulfide conversion. Stage IV is dependent on the rate of oxidation and the activity of iron oxidizing microbes. Rapid oxidation will convert magnetite to hematite and slow oxidation will cause magnetite to transition to hematite with layers of maghemite in-between phases. Note that hematite will reduce to magnetite and reoxidized to maghemite under well-oxidized conditions. Stage V is the weathering of Fe-oxides to FeOOH and the subsequent release of Fe and As into solution as the hydroxides are exposed to water and dissolved. B) Flow diagram of the cycle showing the multi-step path of the creation of sulfides, microbe activity and the conversion of sulfide to oxide and the subsequent hydration and dissolution of FeOOH and the final release of suspended arsenic and iron to ground water.

4.2 Initial Diagenetic Fe-sulfide Formation

4.2.1 Stage I

Sub-microscopic textural and chemical observations via SEM were crucial in determining the evolution of iron sulfides and oxides in the bedrock, which would be the most reasonable natural source of iron and some other metals in the leachate. Thin section analysis of the Austin Chalk bedrock revealed abundant and widely dispersed pyrite grains throughout the samples (Figure 7). SEM analysis indicates the framboids (e.g., raspberry spheres) are a primary texture indicative of biogenic formation in marine environments (Love 1965, Vallentyne 1963, Sweeney et al. 1973), and the likely result from microbial action soon after deposition in the chalk 90 million years ago (Ma). Marine sediments rich in organic carbon (OC) are also usually rich in sulfur and iron and, in fact, much of the iron and nearly all of the sulfur in these sediments are digenetic iron sulfide (FeS) (Dean et al. 1989). Formation of sulfides in these sediments results from microbial reduction of seawater sulfate. Sulfate-reducing bacteria (SRB) assist and then consume OC in the process. These processes are a very well-known response to the development of reducing conditions in the presence of high sulfate and is part of early diagenesis (Neretin et al. 2004).

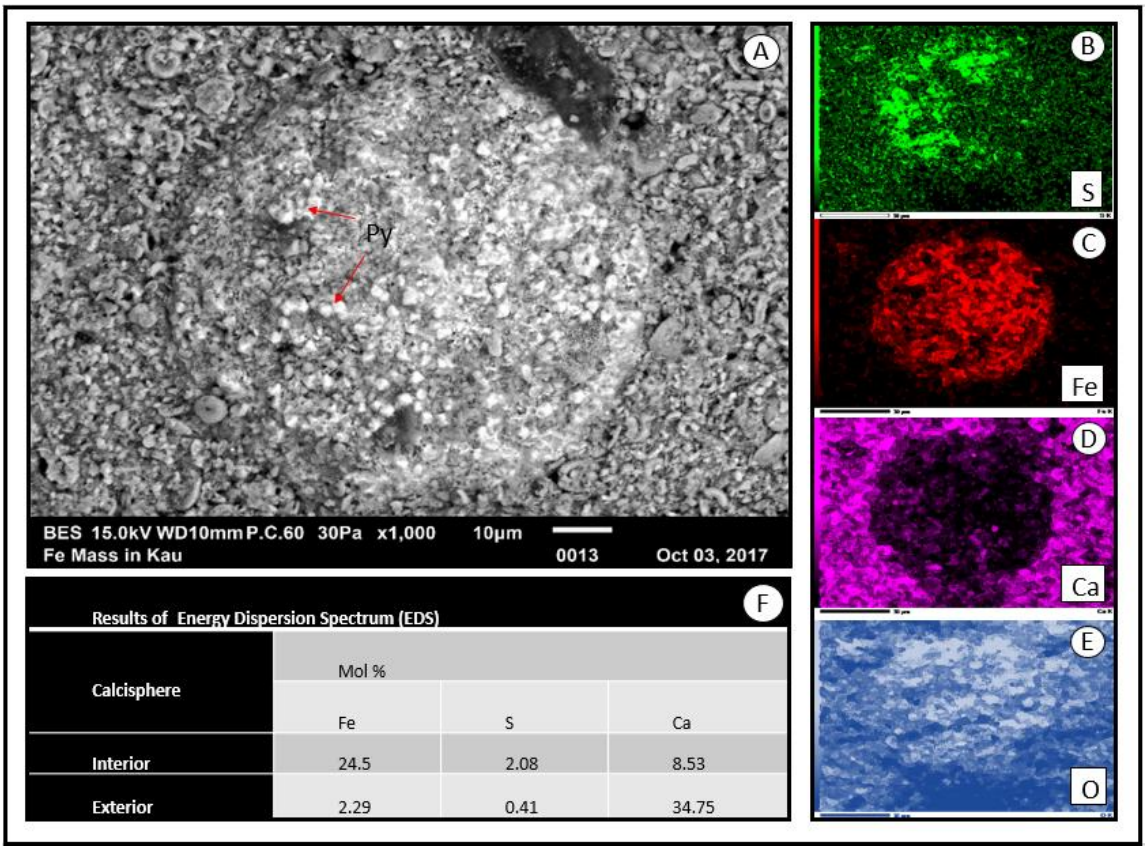

Figure 7: Stage I formation of diagenetic formation of pyrite. A) SEM image at 15 keV showing weathered calcisphere with biogenic pyrite in the interior (Masters and Scott 1978). Scale is 40-60 µm. Matrix is biogenic sediments of coccolithospheres. Panels B-E shows a color intensity map of detected elements with EDS backscatter detector. Panel F is a table of the mol % of the elements detected in the interior vs exterior. The interior is iron-sulfide dominated, while the exterior is carbonate. Precipitation of pyrite occurs simultaneously as the calcite forms around the grains.

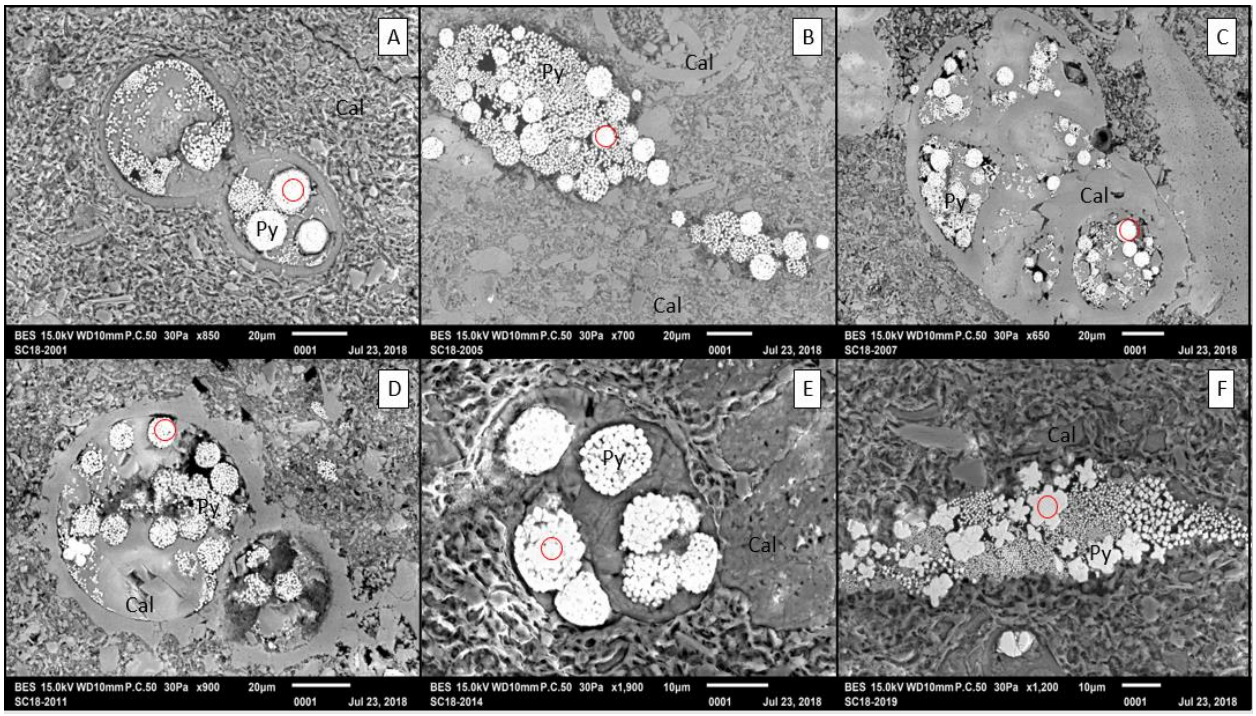

Figure 8: Stage I/II; Biogenic Frambodial pyrite in pore spaces of foraminifera in Austin Chalk. Red circle in panels show points that were analyzed by microprobe. Secondary minerals form within the pore space from the microbial activity of SRB. Scale varies (10µm -20 µm). Microprobe beam was at 20 KeV. Letter in upper corner corresponds to microprobe Analysis ID in Table 5.

Table 5: Stage I/II Results of electron microprobe analysis of unweathered biogenic iron sulfides in pore space in foraminifera (locations shown in Figure 8) Note predominance of iron and sulfur, limited oxygen, and consistently elevated arsenic.

Concentration (wt. % element) normalized to Total = 100%							
Analysis ID	Fe Kα	S Kα	As Lα	Mg Kα	Ca Kα	Mn Kα	O Kα
A	46.46	50.68	0.11	0.44	0.54	0.31	1.45
B	45.40	53.44	0.19	0.43	0.27	0.00	0.28
C	45.44	53.29	0.22	0.43	0.18	0.21	0.23
D	44.73	52.95	0.21	0.44	0.82	0.00	0.82
E	47.74	49.04	0.20	0.46	0.72	0.05	1.79
F	45.08	53.36	0.13	0.43	0.61	0.11	0.27

4.2.2 Stage II

These biogenic Fe-sulfides occur most readily in the forms of pyritized calcispheres, coccolithospheres, and foraminifera, which occur on the death of a microbial colony. Upon diagenesis sediment, accumulation will occur and in the first few centimeters of burial at the sea floor, a calcisphere can form in conditions that use the FeS available in the oxygenated water over an anoxic layer to create biogenic pyrite as the environment becomes more reduced (Wilkin et al. 1996, Wilkin and Barnes 1997). Calcispheres are spherical, calcareous bodies of algal origin in lagoonal limestone and chalks that commonly contain pelagic sediments (Hart 1991; Hart 1993). They can be important stratigraphic and paleoenvironmental indicators (Bonet,

1956; Villain ,1975; Masters et al., 1978). Framboids occur secondarily as the sulfate in seawater is reduced by sulfur reducing bacteria (SRB) and the 'raspberry' texture indicates microbial colony depositions. Mineral compositions of framboids is confirmed from SEM-EDS/microprobe data. Analysis shows high concentrations of Fe localized in the interior and sulfur around the edge of the exposed calcisphere. The absence of aluminum (Al) and calcium (Ca) in the interior in combination with the Fe, Oxygen (O), and Sulfur (S) indicate that the center is mostly pyrite with insitu weathering (Figure 7).

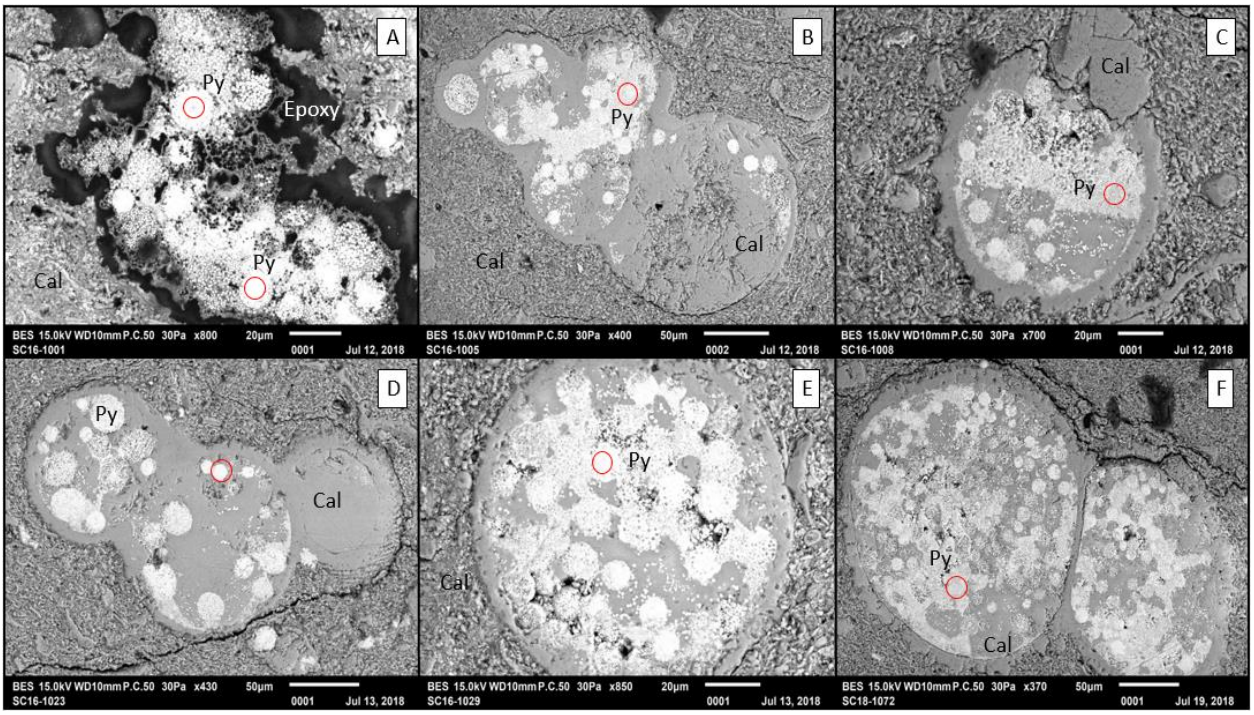

Figure 9: Stage II alteration; Electron microprobe images of foraminifera from seep bedrock that have had pore space pyritized (white areas), multiple cycles of sulfides are seen in the foraminifera with infill of pyrite. Circle (red) in panels show point that was analyzed by microprobe. Scales vary (20 µm - 50µm). Microprobe beam was at 20 KeV. Subfigure designator A-F identifies the corresponding elemental results in Table 6.

Table 6: Stage II; Results of concentrations (electron microprobe) of iron oxides and sulfides that have replaced empty pore-space in bedrock chalk. See point locations in Figure 9. All but A2 are pyrite that has been converted to marcasite or iron oxides (Stage II alteration). Note the slight increase of iron, moderate increase in oxygen, steady levels of Arsenic, and the reduction of sulfur as pyrite decay and secondary mineral growth ensue.

Concentration (wt. % element) normalized to Total = 100%							
Analysis ID	Fe Kα	S Kα	As Lα	Mg Kα	Ca Kα	Mn Kα	O Kα
A1	59.94	0.09	0.11	0.48	0.40	0.00	38.98
A2	44.74	52.22	0.23	0.44	0.88	0.07	1.42
B	62.81	0.09	0.18	0.56	1.31	0.00	34.71
C	58.80	0.04	0.16	0.53	1.76	0.00	38.69
D	62.02	0.04	0.23	0.53	1.43	0.00	35.74
E	60.87	0.03	0.18	0.57	2.32	0.00	36.01
F	60.87	0.05	0.19	0.53	1.37	0.00	36.99

4.3 Intermediate Weathering and Alteration of sulfides to oxides

4.3.1 Stage III

Near-surface breakdown and dissolution of sulfides is presumably the main mechanism for iron and arsenic migration in the streambank leachate. Hence the introduction of high Eh meteoric waters likely breaks down the sulfides (pyrite and marcasite) to magnetite (Brothers et al. 1996), followed by further oxidation to hematite-maghemite (and siderite $FeCO_3$ in carbonate rocks), and finally amorphous iron oxy-hydroxides (e.g., limonite ($FeO(OH)\cdot nH_2O$; Ellwood et al.

1986). Reductive dissolution of FeOOH, which releases arsenic, and under oxidizing condition, e.g., low-temperature groundwater, will bind it (Figure 10; Kinniburgh and Smedley 2012). Prominent iron staining along near surface fractures in the Austin Chalk indicates this process is occurring with reduction of iron and other trace metals (e.g., Coakley Superfund site; DeLemos et al. 2006). Similarly, residual clays left during carbonate dissolution, can accumulate, especially in surface channels, affecting vertical permeability. The process is partly self-sustaining, since release of sulfuric acid (H_2SO_4) occurs with the decay of marcasite in the presence of water, increasing permeability, porosity, and the enhancing the penetration of meteoric water into the formation.

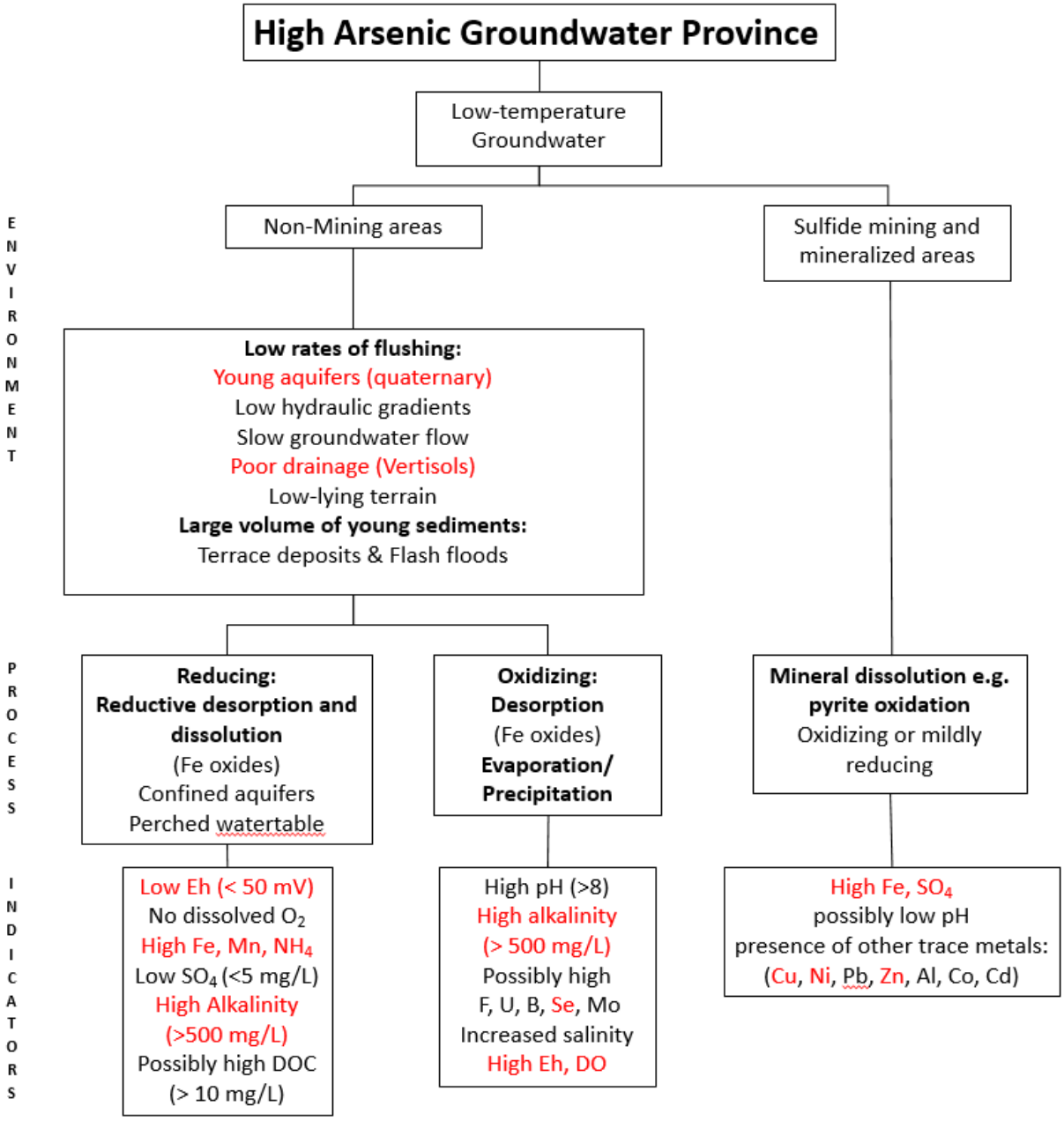

Figure 10: Classification of groundwater environments prone to arsenic problems from natural sources modified from Smedley and Kinniburgh 2002. Not all the indicators of low rates of flushing necessarily apply to all environments. The highlighted sections are values that are present in the study area, Figure 3.

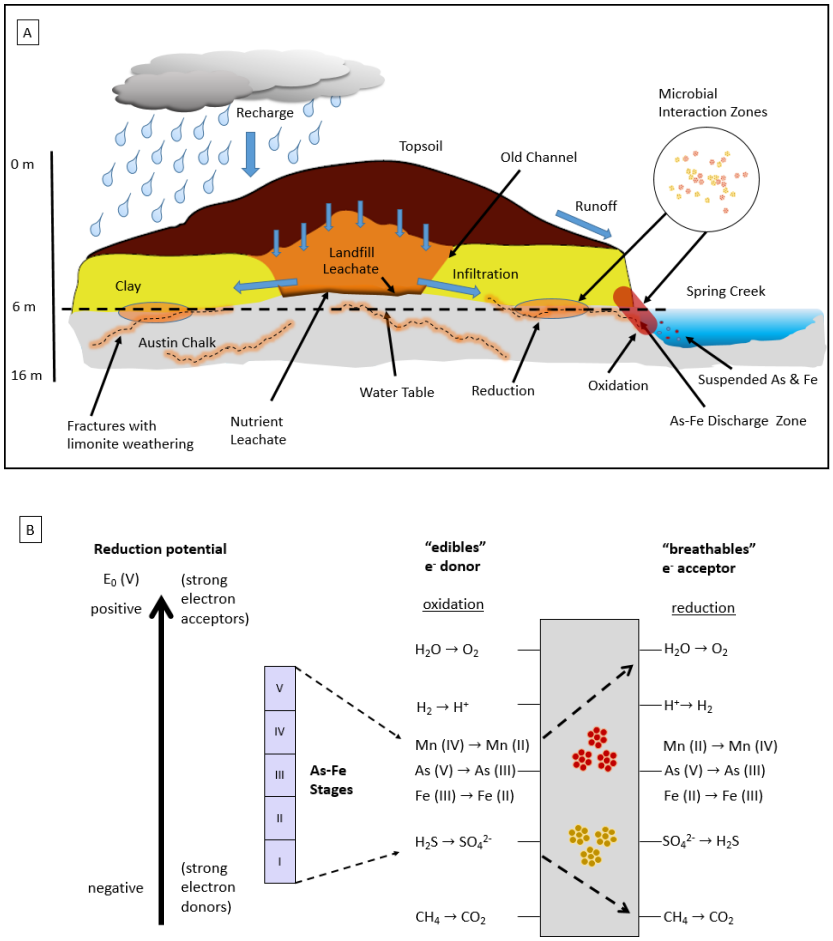

Figure 11: Model of As-Fe transport and microbial interaction zone. A) Spring Creek Reductive Dissolution Cycle: Recharge sinks into topsoil and infiltrates landfill located in an old channel, the hydrologic conductivity (K) >> 0, so the bulk of the recharge enters the landfill and the hydrologic conductivity of the surrounding clays is K< 0 so fluids travel through expansive montmorillonite clays, and interacts with the fractured Austin Chalks (K = 10^-7). Fractures and dissolved pore spaces from iron oxide weathering and pyrite decay allow for microbe populations (e.g., sulfur and iron reducing and oxidizing bacteria) to take nutrients from the landfill and work there natural processes upon the chalk and facilitating the transport of As and Fe (red oval). B) Redox tower of microbial interaction zone and metabolism. Microbes can use a wide range of electron (e^-) donors ("edibles") and electron acceptors ("breathables") to generate energy for metabolism. Potential electron donors and their oxidation products are shown on the left; potential electron acceptors and their reduction products are shown on the right. S and Fe microbes shown in the middle of tower with the main transport of Mn, As, and Fe at work; Reactions of iron oxidation, iron reduction at the top and sulfur oxidation and reduction at the bottom. Strong electron acceptors are shown at the top, strong electron donors on the bottom. Oxidation reactions may occur so long as the reduction reaction of the electron donor is lower than the electron acceptor (the electrons must flow 'downhill').

The full scope of how microbes affect this system is not fully understood, but the roles of iron and sulfur bacteria are facilitators and catalysts to the system as seen in Figure 6. The redox-oxidation cycle is altered as microorganism use and generate energy for metabolism (Figure 11). Submarine bacteria reduced the sulfur in the seawater creating breathable electrons (i.e., acceptors or food for microbes), and during diagenesis helped priduce the framboids (biogenic, Figure 8). Subterranean bacteria (chemotrophs; Biddanda et al. 2011) helped to migrate the sulfur and iron as edibles, which changes the pH, Eh of the system, and surficial bacteria could use the nutrient in the groundwater to further break down the minerals present (siderite, hematite, magnetite, FeOOH).

Iron rich groundwater or sediment porewaters more likely form as a consequence of the action of anaerobic heterotrophic Fe(III)-reducing bacteria, which must come in contact with the solid surface to reduce the Fe(III) and thus preferentially utilize the least crystalline (greater surface area) Fe oxyhydroxide phases (Lovely & Phillips, 1988; Phillips et al.,1993; Roden et al., 1996). This is confirmed for the study area rocks by SEM-EDS, which show that amorphous Fe typically remains after replacing sulfide grains (Figure 13). Microprobe and EDS demonstrate the loss of sulfur and retention of iron is in these areas (Table 7, Figure 12). Ultimately, about 80% of Fe grains are oxides, and dissolution occurs from the edge of the grain toward the center.

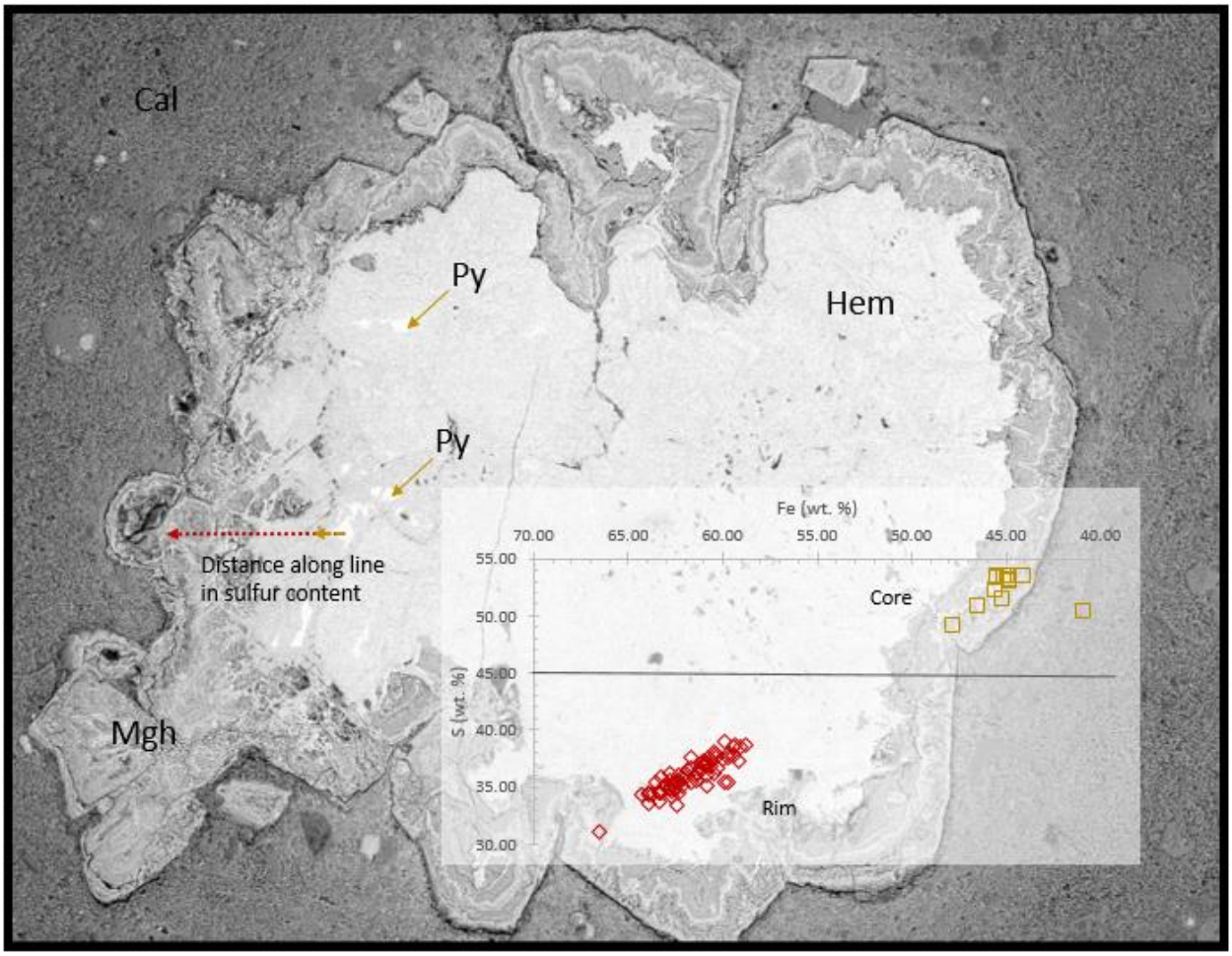

Figure 12: Stage III formation of iron oxide rims on primary pyrite grains. Microprobe analysis of amorphous iron oxides that shows a trend of decreasing sulfur content from iron sulfide grains in the center (yellow arrows and points in inset diagram) to the increase of iron content and loss of sulfur toward the rim. (red points in diagram, taken along red dotted path in photomicrograph) e.g., effectively capturing the breakdown of sulfides into iron oxides).

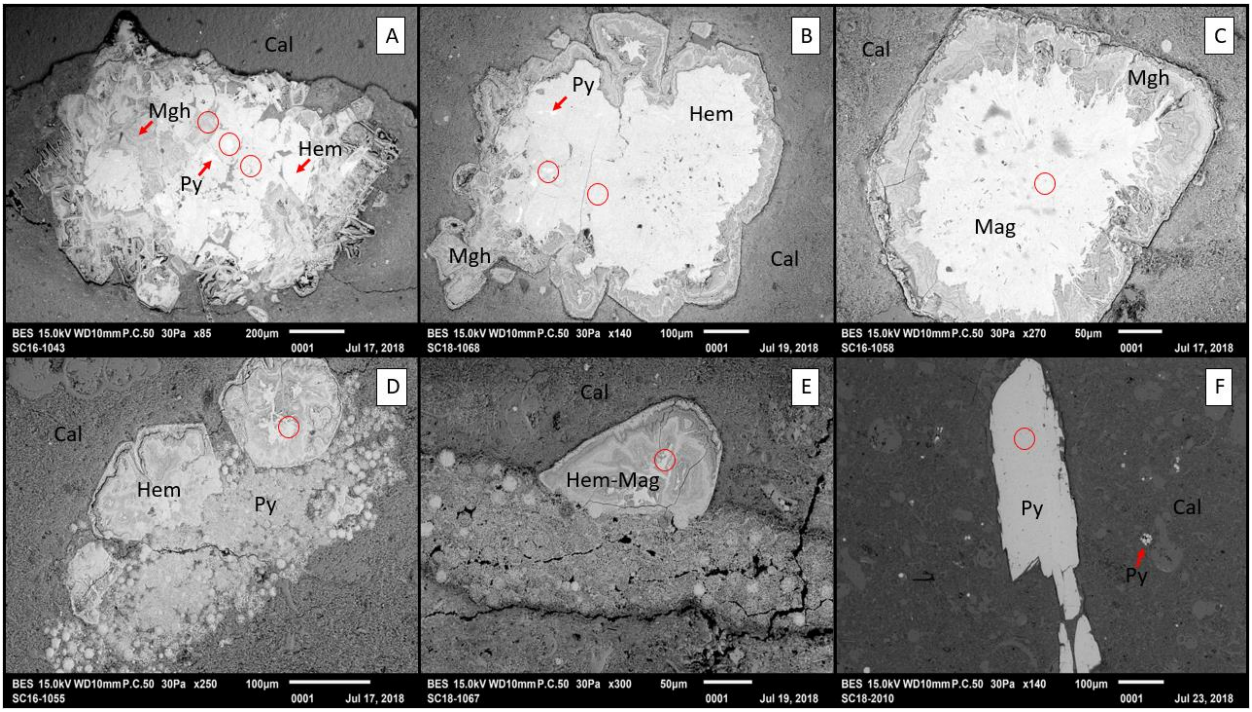

Figure 13: Stage III, formation of amorphous iron oxides that have replaced sulfide grains, demonstrating loss of sulfur and retention of iron in these areas, Dissolution of oxides and colony growth from Fe-OB are present in panel D and E. Red circle in panels show point that was analyzed by microprobe. Scale varies (50 µm- 200 µm). Microprobe beam was at 20 KeV. Subfigure designator A-F identifies the corresponding elemental results in Table 7.

Table 7: Stage III; Results of electron microprobe concentrations of intermediate step of sulfide grains converting to oxides in Austin Chalk. See point locations in Figure 13. All but F have gone through some stage of alteration from sulfide to oxide. Note the slight increase of iron, moderate increase in oxygen, steady levels of arsenic, and the reduction of sulfur in oxides. Sulfides have a lower arsenic content than oxides.

Concentration (wt. % element) normalized to Total = 100%							
Analysis ID	Fe Kα	S Kα	As Lα	Mg Kα	Mn Kα	Ca Kα	O Kα
A1	45.67	53.41	0.06	0.42	0.02	0.02	0.40
A2	63.22	0.07	0.08	0.46	0.00	0.29	35.87
A3	61.68	0.05	0.07	0.48	0.00	0.13	37.58
B1	45.97	52.91	0.09	0.42	0.23	0.00	0.39
B2	64.25	0.10	0.09	0.46	0.31	0.40	34.39
C	63.53	0.07	0.09	0.47	0.01	0.41	35.42
D	62.80	0.07	0.10	0.48	0.00	0.36	36.19
E	59.41	0.25	0.13	0.51	0.00	1.18	38.52
F	0.54	31.32	0.05	1.27	4.38	4.15	57.52

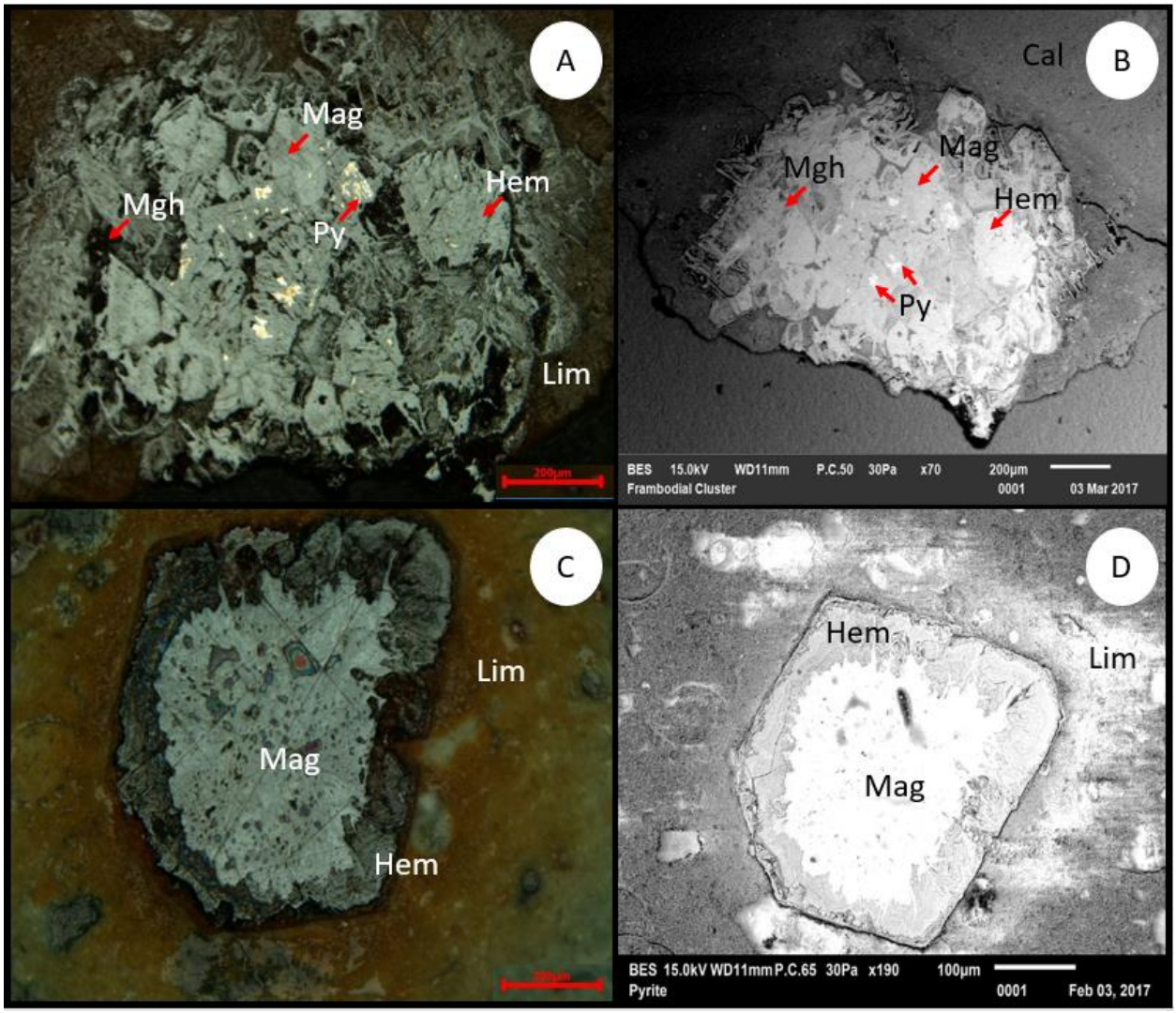

Figure 14: Stage III/IV formation of iron oxides and limonite with residual pyrite core. Reflective and SEM images of alteration in Austin Chalk. Panel A-B shows a hematite/maghemite cluster with a trace amount of pyrite in the center. Scale is 200-µm. Panel C-D show a hematite grain with dissolution of the grain resulting in the conversion of iron oxides converting to Fe hydroxides. Scale is 100-200 µm.

4.4 Source of trace metals: Iron Oxide-Hydroxide Dissolution

4.4.1 Stage IV

Morphological features in the iron sulfides and oxides show strong evidence that the release of certain trace metals (e.g., As, Mn, and Ti) are related to the structure of biominerals. The trace metals and iron are concentrated in the sulfide grains, since they are quickly precipitated in sulfidic sedimentary environments due to extremely low solubility of metal sulfide minerals (Ehrlich, 1996; Saunders et al., 1996). The microprobe demonstrates strong correlation between Fe and As concentrations in all analyzed grains, and FeS and As in initial depositional grains, indicating a suitable source of the seep As is from both the sulfide minerals, and their breakdown products (Fe oxides) that exhibit somewhat more concentrated As (Figure 16).

Three repeatable features are emerging from the SEM observations: A framboidal texture, single or multi-domain crystal habits, and conglomerates of minerals (oxides and sulfides; Figure 8, Figure 13, Figure 15) coupled with microprobe data indicate that three mineral groups are (Fe-carbonates, sulfides, and oxides) are responsible for the enrichment and transport of arsenic (Figure 16) in these seeps. It is likely that the converting of Fe-carbonates and sulfides to the mineral phase alteration cycle of magnetite, maghemite, hematite, goethite, and limonite facilitate the release of trace metals (Correa et al., 2006, Brothers et al., 1996, Ellwood et al., 1986). Predominance of oxides in host rocks indicate that As is released and enriched during this cycle (Stage II/IV, Figure 6). The As is desorbed and released during reductive dissolution of the Fe oxyhydroxies and microbial reduction of the Fe oxyhydroxides by ground water microbes (i.e., FeOB and FeRB; Figure 6, Figure 11). The levels of As vary from low (0.1 to 0.27 wt. %)

to high (0.6 to 1 wt. %) in the Fe sources and are elevated in oxides compared to sulfides (Figure 16).

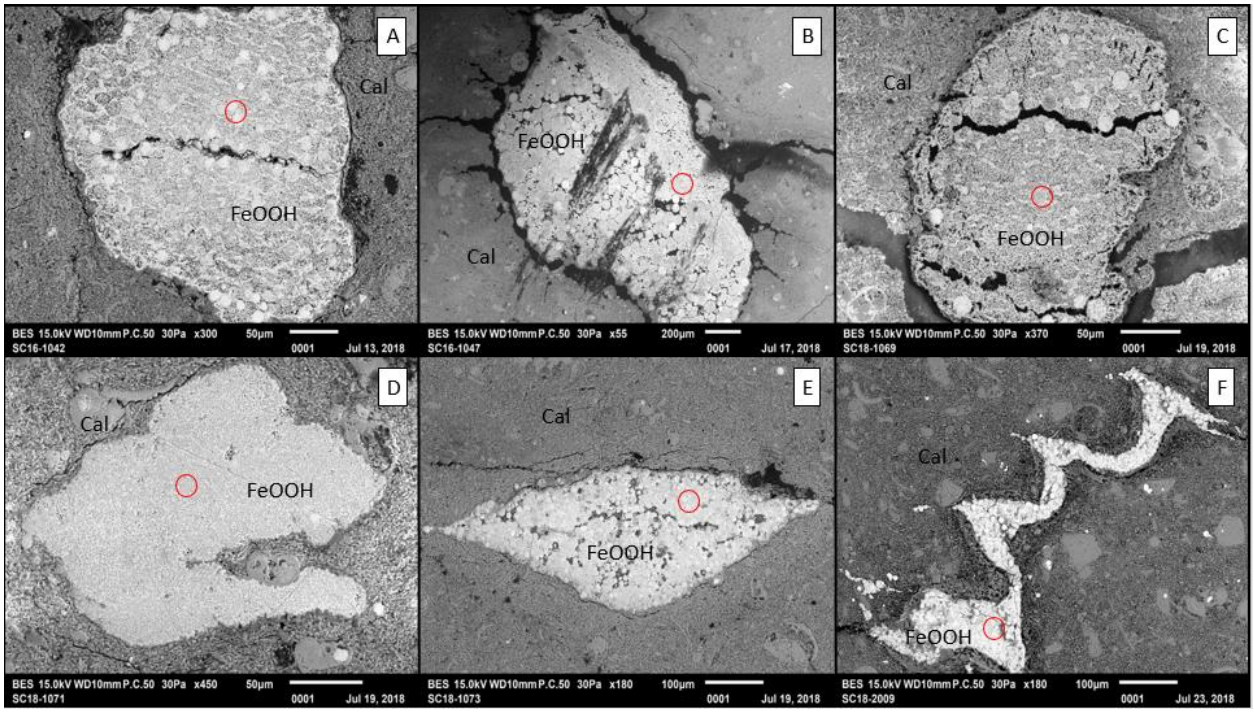

Figure 15: Stage IV/V; Iron oxy-hydroxides that has filled in pore spaces and are fluid conduits for during initial Fe dissolution. Dissolution of oxides and colony growth from Fe oxidizing bacteria are present in all panels. Red circle in panels show point that was analyzed by microprobe. Scale varies (50 µm- 200 µm). Microprobe beam was at 20 KeV. Subfigure designator A-F identifies the corresponding elemental results in Table 8.

Table 8: Stage IV/V; Results of electron microprobe showing element concentrations of weathered amorphous iron hydroxides in Austin Chalk. See point locations in Figure 15. All but F have gone through some stage of alteration from sulfide to oxide. Note further increase of iron, elevated oxygen, and the enrichment of arsenic through the stages I-III. Sulfur is a residual of the pyrite and the microbial activity of SRB and SOB in the subsurface. Arsenic is primed for fluids to dissolve the FeOOH and precipitate suspend Fe and As.

Concentration (wt. % element) normalized to Total = 100%							
Analysis ID	S Kα	Fe Kα	As Lα	Mg Kα	Ca Kα	Mn Kα	O Kα
A	0.37	62.36	0.19	0.50	0.51	0.00	35.96
B	1.99	60.25	0.16	0.50	0.52	0.00	36.59
C	0.25	59.41	0.13	0.51	1.18	0.00	38.52
D	0.13	63.88	0.16	0.57	0.74	0.06	34.46
E	0.07	63.91	0.08	0.58	0.99	0.00	34.36
F	0.08	61.24	0.12	0.56	1.15	0.00	36.57

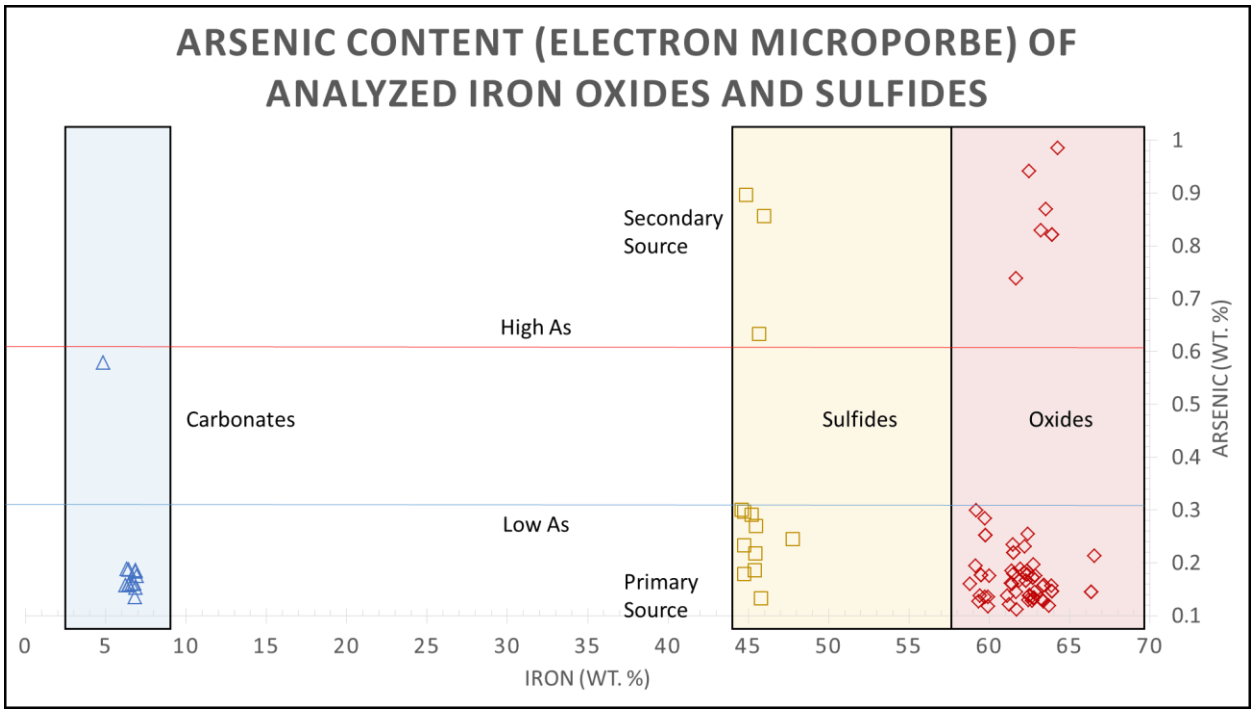

Figure 16: Microprobe results showing the arsenic concentrations plotted against iron concentrations, symbols represent individual analysis of Fe-grains. Note the background signature of 0.15 wt.% As in all grains, elevated values (0.6-1.0 wt. %) believed to be mobilized As. Oxides are the dominate mineral phase being the end result of sulfide and carbonate conversion to $FeOOH_x$. Enrichment of As thought to be shown as it transitioned from mineral phase to mineral phase seems likely in the separation of low to high As values. The concentration of As is primarily in oxides and secondary in sulfides.

4.4.2 Stage V

In aquatic environments, such as oceans, rivers, and sediments, microbes play an important role in the dissolution of minerals. Enhanced dissolution of iron (hyd)oxides becomes more prevalent at the surface with the interaction of soil bacteria and meteoric waters. These microbes help liberate the iron into a state which is more readily transported via ligands and siderphores (i.e., small, high-affinity iron-bonding compounds secreted by microorganisms such as bacteria serving to transport iron across cell membranes), thus significantly increasing the dissolution of FeOOH (Hersman et al. 1996; Hersman 1995). These microbes facilitate Fe uptake in oxic

environments, and influence mineral weathering. In North-Central Texas the groundwater passes through the fractured chalk and interacts with zones of microbe activity (Figure 11), enriching them with iron and arsenic (Figure 16). Emergence of these Fe-As fluids from the stream orifice causes an equilibrium reaction with the atmosphere as it transitions from a reducing to an oxidizing environment, to precipitates the Fe that has been dissolved, indicated by the reduction in TDS and fluctuation of Eh (Figure 17), and creates a reddish brown discharge ($Fe(OH)_3$) along the banks. The levels of detectable arsenic vary considerably depending on sample location along the discharge, e.g., 100 ppb at the orifice and 15 ppb at the stream entry, hence increasing toxicity of the groundwater at the orifice.

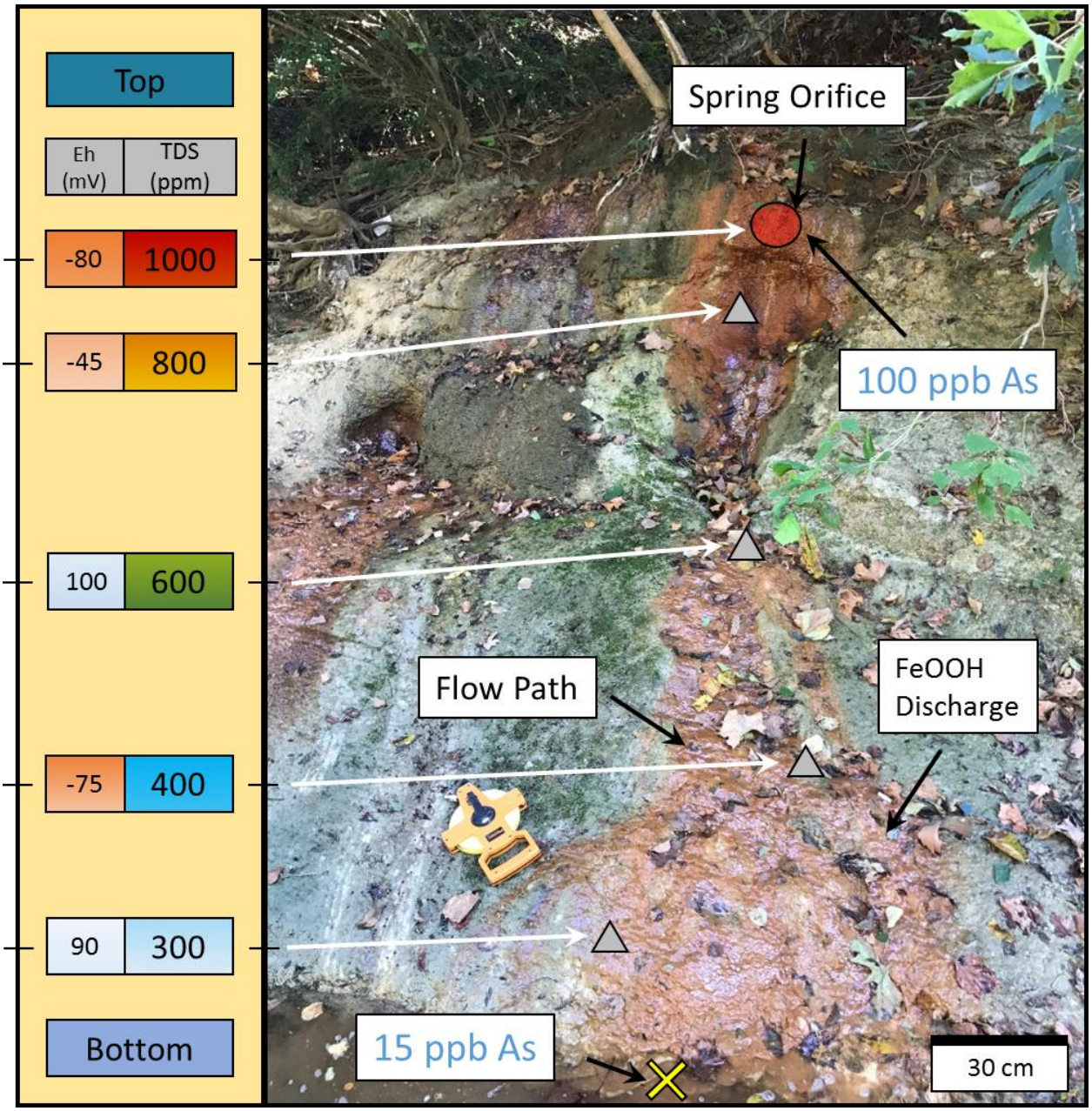

Figure 17: Stage V of As-Fe transport and release showing the Fe staining that is the precipitation of FeOOH coupled with the release of Arsenic as fluids emerge from the country rock and react with atmosphere. (e.g., oxidation fluxes occur with Eh from top to bottom and the TDS steadily declines). Depending on the sampling technique, the amount of Fe and As detected along flow line changes as indicated with the changes in TDS.

CHAPTER 5

DISCUSSION AND CONCLUSION

5.1 Discussion

Despite the strong spatial association between the iron-rich seeps and closed, unlined landfills (Fig. 3a and 3b), water and rock analysis indicates a natural origin for the iron and arsenic. Detailed examination of other creek beds in the area found no other similar concentrated seeps, reinforcing the spatial connection of Fe-As seeps and up-gradient landfills. A possible explanation for the spatial correlation is that the presence of the landfills enhances the subsurface weathering of sulfides in the bedrock chalk outlined in the detailed SEM-EDS and Microprobe results described above. This enhancement might be in surface infiltration, or perhaps more likely via excitation of sulfur reducing bacteria down hydraulic gradient.

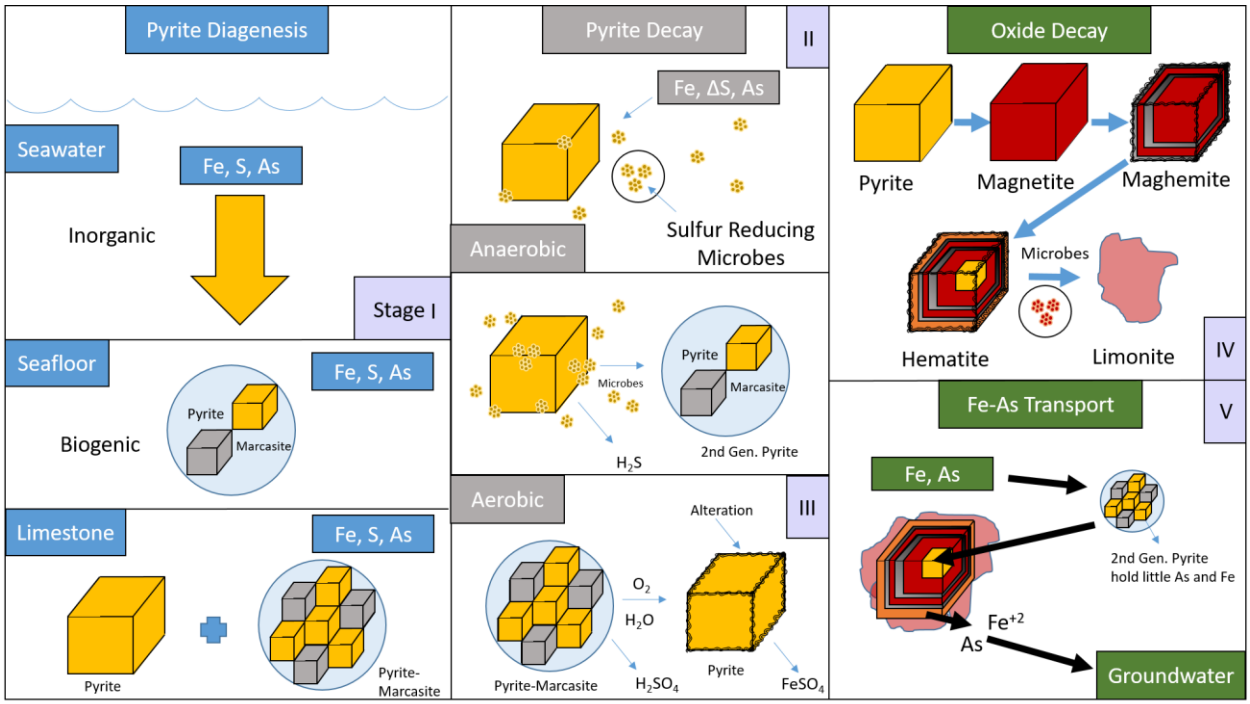

Figure 18: Physical cycle of Fe-As transport and release in Austin Chalk. Stage I is pyrite (inorganic and organic) diagenesis and incorporation of arsenic in the mineral. Stage II is pyrite decay cycle of sulfides. Stage III is the start of reprecipitation-dissolution of sulfides to oxides, small loss of sulfur commences and the secondary formation of Fe-sulfide minerals form, the acid that is release in the pyrite-marcasite decay in stage II allows the pH to lower and help in the dissolution of siderite and sulfide conversion. Stage IV is oxide decay, which is dependent on the rate of oxidation and the activity of iron oxidizing microbes. Rapid oxidation will convert magnetite to hematite and slow oxidation will cause magnetite to transition to hematite with layers of maghemite in-between phase. Note that hematite will reduce to magnetite and reoxidized to maghemite under well-oxidized conditions. Stage V is the weathering of Fe-oxides to FeOOH and the subsequent release of iron and arsenic into solution as the hydroxides are exposed to water and dissolved. Note that process-involving microbes are catalyst to the system and are dynamic.

The source and transport of As is intrinsically linked to the diagenetic formation of the sulfide grains in the chalk. These form under anaerobic conditions during burial as rapid replacement of the calcispheres rich carbon interior is converted to biogenic and inorganic grains (Figure 7 and Figure 18 Stage I). Through compaction and lithification, the foraminifera and other biogenic

sediments are gradually replaced by biogenic sulfides cannibalized from sulfur in the calcispheres (Figure 8). Secondary processes of pyrite decay occur as chalk is exposed to water, and the acid produced in the reaction allows for the dissolution of more pore space and the filling of it with subsequent sulfides or amorphous iron (Stage II & III; also Figure 13 and Figure 15). Simultaneous growth and destruction of sulfides continues as the chalk weathers. As the chalk is exhumed and conditions shift toward oxidation via groundwater infiltration, the sulfide grains start to undergo surface reprecipitation-dissolution (Stage III, and Figure 13). Sulfide grains alter to magnetite and ultimately under increasing Eh and pH (Figure 5) alter to maghemite under slow oxidation or hematite under rapid oxidation (Stage IV and Figure 12). The unstable maghemite, will transition to hematite and finally will alter to clay minerals such as goethite or limonite (Stage III-IV and Figure 13) in this, more easily weathered state. Finally, FeOOH hosts somewhat increased arsenic (relative to the original sulfides, Figure 16), releasing that arsenic and iron as it is destroyed by reductive dissolution (Stage V, Figure 18).

Although arsenic exceeds state and federal limits at the orifice of the seeps, the above-limit As appears to result from some unidentified enhancement of natural oxidation thought to have some spatial contribution by the overlying legacy landfills. This enhancement may be some sort of perturbation of microbial populations to enhance subsurface weathering As bearing minerals or reinforcement of reducing conditions in the subsurface. Ultimately, formation of these iron-arsenic seeps appears to be a primarily natural process masquerading as direct anthropogenic contamination. Any anthropogenic effects on these seeps appear to be indirect.

5.2 Conclusions

Ultimately, this study reveals an unanticipated hazard of sequential land use in this area and suggests that similar hazards may be present in any area with poorly-lined landfills atop sulfide-bearing materials. In this and any other such case, greater care in landfill cover design may suffice to mitigate hazards like these, and is crucial if the follow-on landuse involves continual irrigation, (e.g., the athletic fields in this case). The natural mobilization of Fe is from the host rock (iron oxides and FeS_2), and the microbes activity (Fe-OB and Fe-RB). Initially, ancient bacteria had a role in the creation of the pyrite and modern bacteria (SOB and SRB) have a role in pyrite dissolution. Fe transport is encouraged by the strong reducing conditions and a positive feedback loop of the decay of sulfides help maintain the conditions.

Due to the enrichment of As from a diagenetic setting the hazard is enhanced by the chemical and physical weathering of sulfides to oxides due to the nutrient from the landfill. Knowing the concentration of As is important to establish a baseline for how much As is transported to the stream systems. Sampling techniques (e.g., at the orifice, down the bank, near the stream) affect this value and make it challenging to estimate the toxicity of As in drinking water. Trace metals are mobilized in iron systems and the contributions from landfills is not fully understood, but the implications to what more anthropogenic sources of contamination mean to a natural system can only be intensified as the breakdown of As bearing minerals increase.

The Austin Chalk has variability dependent on region of the formation but was formed by biogenic activity, and is still being worked upon by biologic activity, and as urban centers

become more populated, the need for more landfills increase. It is important to established practices and plans to deal with possible geogenic hazards. Sequential land use is good, but better engineered fluid paths will reduce the anthropogenic contribution from the landfills to the microbial populations in the country rock. Current regulations mitigate problems like this, but solutions to future problems caused by old methods may improve remediation by having a better cap design. A simple two cap system would allow fluids to permeate the subsurface (to allow for irrigation drainage), but not to let them encounter the landfill. Physical proximity to potential waste initially suggests an anthropogenic link to the discharge zones, details of geology and fluid chemistry indicate this is primarily a natural process in the areas that this study focused on.

Future work may determine the type of microbe that favors this condition (e.g., nutrient rich leachate microbes) and the geometry of potential old channels from the meandering stream to offer controls on fluid pathways and concentration of trace metals in the discharge zones. There is sufficient water flow through the fractured bedrock to create an environment that allows the subsurface microbes (SRB and SOB) to enhance the dissolution of iron bearing minerals and subsequently transport the dissolved metals and trace elements. In short, this Fe-As discharge looks and smells nasty and is an eyesore to the public, but it is in general natural and does not present an environmental or health hazard.

REFERENCES

[1] "Closed Landfill Inventory." Transportation Systems Management (TSM) - NCTCOG.org. Accessed August 21, 2018. https://www.nctcog.org/envir/materials-management/closed-landfill-inventory.

[2] "National Primary Drinking Water Regulations." EPA. March 22, 2018. Accessed November 26, 2018. https://www.epa.gov/ground-water-and-drinking-water/national-primary-drinking-water-regulations.

[3] Apgar, M. A., and Langmuir, D. "Ground-Water Pollution Potential of a Landfill Above the Water Tablea." *Ground Water* 9, no. 6 (1971): 76-96. doi:10.1111/j.1745-6584.1971.tb03582.x.

[4] Biddanda, B. A., Nold, S. C., Dick, G. J., Kendall, S. T., Vail, J. H., Ruberg, S. A. & Gre en, C. M. (2011) Rock, Water, Microbes: Underwater Sinkholes in Lake Huron are Habitats for Ancient Microbial Life. Nature Education Knowledge 2(12):9.

[5] Brothers, L. A., Engel, M. H., and Elmore, R. D. "The Late Diagenetic Conversion of Pyrite to Magnetite by Organically Complexed Ferric Iron." *Chemical Geology* 130, no. 1-2 (1996): 1-14. doi:10.1016/0009-2541(96)00007-1.

[6] Correa, J. R., Canetti, D., Castillo, R., Llópiz, J. C., and Dufour, J. "Influence of the Precipitation PH of Magnetite in the Oxidation Process to Maghemite." *Materials Research Bulletin* 41, no. 4 (2006): 703-13. doi:10.1016/j.materresbull.2005.10.009.

[7] Dean, W. E., and M. A. Arthur. "Iron-sulfur-carbon Relationships in Organic-carbon-rich Sequences; I, Cretaceous Western Interior Seaway." *American Journal of Science* 289, no. 6 (1989): 708-43. doi:10.2475/ajs.289.6.708.

[8] DeLemos, J. L., Bostick, B. C., Renshaw, C. E., Stürup, S., and Xiahong, F. 2006. "Landfill-Stimulated Iron Reduction and Arsenic Release at the Coakley Superfund Site (NH)." *Environmental Science and Technology* 40 (1): 67–73. doi:10.1021/es051054h.

[9] Drever, J. I. 1988. Geochemistry of natural water, 2nd ed. Englewood Cliffs, NJ: Prentice Hall.

[10] Ehrlich, H. L. "Manganese Oxide Reduction as a Form of Anaerobic Respiration." *Geomicrobiology Journal* 5, no. 3-4 (1987): 423-31. doi:10.1080/01490458709385977.

[11] Ellwood, B. B., Balsam, W., Burkart, B., Long, G. J., and Buhl, M. L. "Anomalous Magnetic Properties in Rocks Containing the Mineral Siderite: Paleomagnetic Implications." *Journal of Geophysical Research: Solid Earth* 91, no. B12 (1986): 12779-2790. doi:10.1029/jb091ib12p12779.

[12] Fungaroli, A. A. and Steiner, R. L. "Laboratory study of the behavior of a sanitary landfill." J. Wat. Pollut. Control Fed., 43 (1971), pp. 252-267.

[13] Hart, M. B., Dodsworth, P., and Duane, A. M. "The Late Cenomanian Event in Eastern England." *Cretaceous Research* 14, no. 4-5 (1993): 495-508. doi:10.1006/cres.1993.1035.

[14] Hersman, L., Lloyd, T., and Sposito, G. "Siderophore-promoted Dissolution of Hematite." *Geochimica Et Cosmochimica Acta* 59, no. 16 (1995): 3327-330. doi:10.1016/0016-7037(95)00221-k.

[15] Hersman, L., Maurice, P., and Sposito, G. "Iron Acquisition from Hydrous Fe(III)-oxides by an Aerobic Pseudomonas Sp." *Chemical Geology* 132, no. 1-4 (1996): 25-31. doi:10.1016/s0009-2541(96)00038-1.

[16] Kjeldsen, P., Barlaz, M. A., Rooker, A. P., Baun, A., Ledin, A., Christensen, T. H., 2002. "Present and long term composition of MSW landfill leachate—a review." Crit. Rev. Environ. Sci. Technol. 32, 297–336.

[17] Love, L. G. "Micro-Organic Material With Diagenetic Pyrite From The Lower Proterozoic Mount Isa Shale And A Carboniferous Shale." *Proceedings of the Yorkshire Geological Society* 35, no. 2 (1965): 187-202. doi:10.1144/pygs.35.2.187.

[18] Lovley, D. R., and Phillips, E. J. P. "Novel mode of microbial energy metabolism: organic carbon oxidation coupled to dis- similatory reduction of iron or manganese." Appl. Environ. Microbiol., 54 (1988): 1472–1480.

[19] Masters, B. A., and Scott, R. W. "Microstructure, Affinities and Systematics of Cretaceous Calcispheres." *Micropaleontology* 24, no. 2 (1978): 210. doi:10.2307/1485249.

[20] Merz, R.C. "Final report on the investigation of leaching of a sanitary landfill." Calif. State Wat. Pollut. Control Bd. Pub., 10 (1954), p. 92.

[21] Neretin, L. N., Böttcher, M. E., Jørgensen, B. B., Volkov, I. I., Lüschen, H., and Hilgenfeldt, K. "Pyritization Processes and Greigite Formation in the Advancing Sulfidization Front in the Upper Pleistocene Sediments of the Black Sea." *Geochimica Et Cosmochimica Acta* 68, no. 9 (2004): 2081-093. doi:10.1016/s0016-7037(03)00450-2

[22] Panno, S. V., Hackley, K. C., Hwang, H. H., Greenberg, S. E., Krapac, I. G., Landsberger, S. and Okelly, D. J. "Characterization and Identification of Na-Cl Sources in Ground Water." *Ground Water* 44, no. 2 (2006): 176-87. doi:10.1111/j.1745-6584.2005.00127.x.

[23] Phillips, E., Lovley, D. R., and Roden, E. E. (1993) "Composition of non-microbially reducible Fe(III) in aquatic sediments." Appl. Environ. Microbiol. 59, 2727–2729.

[24] Qasim, S. R., and Burchinal, J. C. "Leaching from simulated landfills." J. Wat. Pollut. Control. Fed., 42 (1970), pp. 371-379.

[25] Roden, E. E. and Zachara, J. M. 1996. "Microbial reduction of crystalline iron(III) oxides: influence of oxide surface area and potential for cell growth." *Environ Sei Technol*, 30: 1618–1628.

[26] Saunders, J. A., and Swann, C. T. "Nature and Origin of Authigenic Rhodochrosite and Siderite from the Paleozoic Aquifer, Northeast Mississippi, U.S.A." *Applied Geochemistry* 7, no. 4 (1992): 375-87. doi:10.1016/0883-2927(92)90027-z.

[27] Saunders, J. A., Pritchett, M. A., and Cook, R. B. "Geochemistry of Biogenic Pyrite and Ferromanganese Coatings from a Small Watershed: A Bacterial Connection?" *Geomicrobiology Journal* 14, no. 3 (1997): 203-17. doi:10.1080/01490459709378044.

[28] Smedley, P. L, and Kinniburgh, D. G. "A Review of the Source, Behaviour and Distribution of Arsenic in Natural Waters." *Applied Geochemistry* 17, no. 5 (2002): 517-68. doi:10.1016/s0883-2927(02)00018-5.

[29] Sweeney, R. E., and Kaplan, I. R. "Pyrite Framboid Formation; Laboratory Synthesis and Marine Sediments." *Economic Geology* 68, no. 5 (1973): 618-34. doi:10.2113/gsecongeo.68.5.618.

[30] Texas Commission on Environmental Quality (TCEQ). *Xenco Lab Analytical Report 344659*. Dallas, TX: Texas Commission on Environmental Quality, Sept. 2009. SMU. 1-14.

[31] Texas Commission on Environmental Quality (TCEQ). *Xenco Lab Analytical Report 353828*. Dallas, TX: Texas Commission on Environmental Quality, Investigation 784269. Dec. 2009. 1-24.

[32] Vallentyne, J. R. "Isolation Of Pyrite Spherules From Recent Sediments." *Limnology and Oceanography* 8, no. 1 (1963): 16-30. doi:10.4319/lo.1963.8.1.0016.

[33] Wilkin, R. T., and Barnes, H. L. "Formation Processes of Framboidal Pyrite." *Geochimica Et Cosmochimica Acta* 61, no. 2 (1997): 323-39. doi:10.1016/s0016-7037(96)00320-1.

[34] Wilkin, R. T., Barnes, H. L., and Brantley, S. L. "The Size Distribution of Framboidal Pyrite in Modern Sediments: An Indicator of Redox Conditions." *Geochimica Et Cosmochimica Acta* 60, no. 20 (1996): 3897-912. doi:10.1016/0016-7037(96)00209-8.

[35] Williams, D. L. "Interaction between landfill leachates and carbonate derived residual soils." A.M. Thesis, University of Missouri (1974), p. 99.

BIOGRAPHICAL SKETCH

Jackie D. Horn was born in Hereford, Texas in 1986 and has lived in Dallas, Texas since 1999. In 1989 Jackie was diagnosed with Charcot Marie Toothe Disease (CMT), a neuromuscular dystrophy, a debilitating disease that will one day render him immobile. He has not allowed this disease to inhibit him, and has instead used it as a means of motivation. Through his motivation to become a geoscientist he earned a B.S. in Geosciences from The University of Texas at Dallas in 2016. An extensive undergraduate research project soon developed into a master's thesis beginning in 2015. Throughout his academic career he has participated in professional geoscience conferences and gathered rewards and accolades within his field of study. Jackie's resourcefulness has awarded him the opportunity to continue his education to the PhD level in Exobiology.

CURRICULUM VITAE

Jackie D. Horn

Address: Dallas, TX

Research Interest

I have an interest in bio-mineralization and the subsequent reactions that cause various elements or the composition of the host rock to change. It is fascinating to delve into understanding the water-rock interaction that microbes play and the means of how a bacterium creates biogenic minerals. My current research is studying the anthropogenic and natural components of landfill-promoted dissolution of pyrites (sulfides) in Cretaceous Chalk. The bacteria (sulfur oxidizing and iron reduction) that are present in the host rock and fluids are most likely the control on the environment (paleo-proxies for production of pyrite), as well as the mobilization of As and Fe in the system. Tools used to probe this line of inquiry that I am familiar with are XRD, XRF, X-ray CT, SEM, Microprobe, MS-ICP (RCRA-8), organic and inorganic chemical analysis (major cations and anions), and IP and DC Resistivity surveys. I would very much like to work on problems like these in the future that use multidiscipline approaches, and new analytical techniques to solve these complex systems.

Academic Course Work

- GEOS 5V08 Special Topics in Geosciences; Paleo-magnetism and Applied Geoscience--A
- GEOS 8V10 Research: Hydrogeology and Environmental Geoscience—A
- GEOS 7110 Environmental Workshop--A
- GEOS 6398 Thesis--A
- GEOS 5V08 Special Topics in Hydrologic Research—A
- GEOS 5V08 Special Topics in Geosciences; Water-Rock Interactions Modeling--A
- GEOS 5V08 Special Topics in Geosciences; Sediments and Strata--A
- GEOS 5V08 Special Topics in Geosciences; Hydrology Research--A
- GEOS 5V08 Special Topics in Geosciences; Hydrology Research--A
- GEOS 5V08 Special Topics in Geosciences; Hydrogeology Research--A
- GEOS 5V08 Special Topics in Geosciences; Electron Microprobe Research--A
- GEOS 5387 Applied Geophysics--B
- GEOS 5384 Ground Penetrating Radar--B+
- GEOS 5375Tectonics—A-
- GEOS 5325 Remote Sensing Fundamentals—B+
- GEOS 5315 The Earth: An Overview—A-

- GEOS 5311 Applied Groundwater Modeling—A
- GEOS 4V08 Special Topics Geology II; Mineral Independent Geothermal Migration—A+
- GEOS 4V08 Special Topics Geology II; Chemistry of Potential Landfill Leachate—A+
- GEOS 4430 Hydrogeology & Aqueous Geochemistry—A-
- GEOS 4369 Volcanic Successions—A
- GEOS 4322 The Earth Systems--C
- GEOS 4320 Physics & Chemistry of Solid Earth—B
- GEOS 4300 Field Geology II—A
- GEOS 3470 Structural Geology—C
- GEOS 3470 Paleo-biology—C+
- GEOS 3464 Igneous & Metamorphic Petrography—B
- GEOS 3421 Stratigraphy & Sedimentology—C+
- GEOS 3310 Environmental Geology—B
- GEOS 3300 Field Geology I—B
- GEOS 2306 Geodesy & Geospatial Analysis—B+

Awards

- Schwartz Opportunity Scholarship, UT Dallas 2018
- Graduate Geosciences Fund Award, UT Dallas 2017
- James L Carter Endowment Fund, UT Dallas 2017
- Gaynor Opportunity Scholarship, UT Dallas 2017
- Honorable Mention at GSA Research Poster Contest 2017
- Aqueous Geochemistry Fund Award, UT Dallas 2015
- Pioneer Scholarship, UT Dallas 2015-2018
- Undergraduate Research Award, UT Dallas 2015
- Summer Field Research Award, UT Dallas 2014 and 2015
- Phi Theta Kappa Scholarship, UT Dallas 2012-2013
- Dean's List, Brookhaven College 2010-2013

Extra-Curricular Activities

- American Association of Petroleum Geologist (AAPG) Student Chapter (2016-2018)
  - **Secretary—**Detailed minuets of the club meetings and activities
- American Institute of Professional Geologist (AIPG) Student Chapter (2018)
  - **President—**Founder and Creator of Club
- Member of Geological Society of America (GSA), 2016-2018
  - Regional Meeting Technical Session and Field Trip Planning, Mar 2019
- Member of American Geophysical Union (AGU), 2017-2018
- Member of American Institute of Professional Geologist (AIPG), 2018
- Member of Dallas Geological Society (DGS), 2018
- Member of Association of Environmental and Engineering Geologist (AEG), 2018
- UTD Tennis Club, 2014-2017
- UTD Geo Club, 2013-2018
- Phi Theta Kappa, Brookhaven Community College, 2010-2013

- Brookhaven String Ensemble – Cello, 2011-2012

Skills

- Well water testing (beeper tape, slug test, well pumping, geotechnical soil test), Piper Diagrams, handheld XRF, XRD, X-ray CT tomography, TerraSpec Halo (IR), MS-ICP, Microprobe and SEM training.
- Leadership, mentoring, organization, management and proficient communication
- Computer Skills: Microsoft Office, Python, Matlab, Aqtesolv, Geochemist Workbench (GWB), Spectra, MODFLOW, PHREEQC, Groundwater Modeling Systems (GMS) AGI Earth Imager 2D, JADE, InTouchScope, XRF Niton Data Transfer (NTD), ERDAS Image 2014, and ArcMap GIS
- Critical thinking, theory and analysis
- Prepare accurate records and reports
- Proactive in problem solving and work environments
- Laboratory experience with chemistry (prep, preservation, and develop methodologies), petrological microscope, granular analysis, and microfossil plate mounting
- Field Experience; Phase one site assessment, soil profiles, field mapping (stratigraphic columns/units, paleo-environment reconstructions), water sampling (Eh, pH, Hardness, TDS, RCRA metals), mineral and fossil identification, photogrammetry, ground penetrating radar (GPR), resistivity and gravity surveys.

Ongoing Educations and Presentations

- **Research Poster at National GSA 2018, Indianapolis, IN**
  Origin of Elevated Arsenic in Possible Landfill Leachate in the Austin Chalk, North Texas: Biogenic reduction of Authigenic Iron Sulfides?
- **Invited Session Theme Presentation at South Central GSA 2018, Little Rock, AR**
  Composite Landfill and Natural Biogenic Leachate Discharge from the Austin Chalk, North Texas
- **Research Poster at National GSA 2017, Seattle, WA**
  Landfill-promoted dissolution of Pyrite/Marcasite (Sulfides) in Cretaceous Chalk
- **Research Poster at South Central GSA 2017, San Antonio, TX**
  Natural or anthropogenic origin for urban iron-rich seepage from the Austin Chalk? Evidence from SEM/EDS
- **Research Poster at GIS Day 2017, Dallas, TX**
  Geochemical Fingerprinting with Energy Dispersive X-ray Spectrometry (SEM-EDS) of intermittent low flux leachate originating from iron sulfide bearing biogenic sediments of the Austin Chalk under gleyic conditions
- **Research Poster at South Central GSA 2016, Baton Rouge, LA**
  Geochemical Fingerprinting with Handheld X-Ray Fluorescence (XRF) of Potential low flux Landfill Leachates

Employment History

June 2015 to April 2017	Vet Tech Assistant	North Tollway Pet Hospital, Dallas, TX
Sept 2013 to May 2015	AVID Tutor	Plano ISD, Plano, TX
Oct 2009 to Sept 2013	Merchandise Team Lead	Macys, Plano, TX
Apr 2009 to Aug 2009	Cirquador Team Lead	Cirque Du Soleil Kooza, New York, NY

Education

May 2016	B.S. in Geoscience	The University of Texas at Dallas, Richardson, TX
Dec 2018	Masters in Geoscience; Hydrology and Aqueous Geochemistry	The University of Texas at Dallas, Richardson, TX